



HAL
open science

New palaeomagnetic results from the Oslo Graben, a Permian Superchron lava province

M.M. Haldan, M.J.M. Meijers, C.G. Langereis, B.T. Larsen, H. Heyer

► **To cite this version:**

M.M. Haldan, M.J.M. Meijers, C.G. Langereis, B.T. Larsen, H. Heyer. New palaeomagnetic results from the Oslo Graben, a Permian Superchron lava province. *Geophysical Journal International*, 2014, 199 (3), pp.1554 - 1571. 10.1093/gji/ggu351 . hal-01854921

HAL Id: hal-01854921

<https://hal.science/hal-01854921>

Submitted on 8 Nov 2021

HAL is a multi-disciplinary open access archive for the deposit and dissemination of scientific research documents, whether they are published or not. The documents may come from teaching and research institutions in France or abroad, or from public or private research centers.

L'archive ouverte pluridisciplinaire **HAL**, est destinée au dépôt et à la diffusion de documents scientifiques de niveau recherche, publiés ou non, émanant des établissements d'enseignement et de recherche français ou étrangers, des laboratoires publics ou privés.



Distributed under a Creative Commons Attribution 4.0 International License

New palaeomagnetic results from the Oslo Graben, a Permian Superchron lava province

M.M. Haldan,¹ M.J.M. Meijers,^{2,3} C.G. Langereis,¹ B.T. Larsen⁴ and H. Heyer⁵

¹Paleomagnetic Laboratory Fort Hoofddijk, Utrecht University, Budapestlaan 17, 3584 CD Utrecht, the Netherlands

²Observatoire de la Côte d'Azur, Faculté des Sciences, Université de Nice-Sophia Antipolis, Géozur UMR7329, bat. 1 250 rue Albert Einstein, Sophia-Antipolis, F-06560 Valbonne, France. E-mail: mmeijers@umn.edu

³Department of Earth Sciences, University of Minnesota, 291 Shepherd Labs, 100 Union Street SE, Minneapolis, MN 55455, USA

⁴Det Norske Oljeselskap, P.O. Box 2070 Vika, 0125 Oslo, Norway

⁵Fjordveien 27, 3080 Holmestrand, Norway

Accepted 2014 September 8. Received 2014 September 4; in original form 2014 April 7

SUMMARY

We have performed an extended palaeomagnetic study of the Oslo Graben volcanics, compared to the study of half a century ago by van Everdingen, using modern techniques and a four times larger amount of sites, plus additional rock magnetic experiments. We conclude that the average direction ($D = 204.0$, $I = -37.9$, $k = 46.9$, $\alpha_{95} = 2.0$) and associated palaeomagnetic pole ($\lambda = 48.3$, $\phi = 155.5$, $K = 52.2$, $A_{95} = 1.9$) of the Krokskogen and Vestfold volcanics together are statistically identical to those of the earlier study. This gives confidence in the fact that older palaeomagnetic studies can be reliable and robust, even though methods have improved. Our larger number of samples, and better age constraints, enable us to separate the data into two major intervals: the younger, on average, Krokskogen area and the older Vestfold area. The results show firstly that palaeolatitudes are slightly higher than predicted by the latest apparent polar wander path (APWP) for Eurasia by Torsvik *et al.* These data support an early Permian Pangaea A configuration and do not necessitate a Pangaea B configuration.

The larger data set also allows us to assess the distribution of the characteristic remanent magnetization directions of the Oslo Graben in terms of geomagnetic field behaviour, which were acquired during a long period of dominantly single polarity the Permo–Carboniferous Reversed Superchron (PCRS). The distributions show a significantly lower virtual geomagnetic pole (VGP) scatter at the observed (low) latitudes than expected from a compilation from lavas of the last 5 Myr. The data do however show excellent agreement with the scatter observed both during the Cretaceous Normal Superchron and the PCRS. A comparison of the directional distributions in terms of elongation is less discriminating, since the large errors in all cases allow a fit to the predicted elongation/inclination behaviour of the TK03.GAD model.

Key words: Palaeomagnetic secular variation; Palaeomagnetism applied to tectonics; Europe.

1 INTRODUCTION

The Earth's magnetic field is produced by a geodynamo process in the molten outer core of our planet. It varies dramatically at various timescales, becoming stronger and weaker and occasionally reversing its polarity altogether. The geomagnetic field plays a crucial role, not only in providing a means of navigation for humans and other species, but also in protecting the Earth's surface and atmosphere from the solar wind and cosmic radiation. It is important to study variations in the Earth's magnetic field in detail because they reveal core and core–mantle boundary (CMB) processes taking place in the deepest Earth. Short-term variations of the magnetic field are studied using data obtained by magnetic observatories and satellites.

Longer term variations are preserved in rocks, which can contain reliable records of the direction and intensity of the magnetic field at the time of their formation. Palaeomagnetic measurements from these rocks allow us to study the variations of the field over thousands, millions, or even billions of years. Changes that might have affected the geodynamo over these very long timescales include the nucleation and growth of the solid inner core and convective processes of the liquid outer core, as well as CMB processes. Recent studies have used numerical models to try and understand how these changes might have affected the geodynamo.

The geomagnetic field undergoes internally (core) driven variations on timescales of less than $\sim 10^4$ yr. The nature of these variations may change through time, depending on longer timescale deep

Earth processes. Palaeomagnetic measurements can be used to define how palaeosecular variation has varied over millions to billions of years. Measurements of the geomagnetic field direction may be converted into virtual geomagnetic poles (VGPs) by assuming that the field on average is a simple geocentric axial dipole (GAD). The distribution of VGPs recorded at specific sites is approximately circular (e.g. Tauxe & Kent 2004; Tauxe & Kodama 2009; Deenen *et al.* 2011). The calculated angular standard deviation (asd, or S) of this VGP distribution and the dependence of S on the locality's palaeolatitude (λ) can be used to describe PSV at any chosen time interval during the geological past (McFadden *et al.* 1991). PSV analyses, therefore, have proven useful to indicate dynamo stability (Biggin *et al.* 2008a; Haldan *et al.* 2009).

Here we present a PSV analysis of the Oslo Graben lava flows that were sampled in the Krokskogen area NW of Oslo and in the Vestfold area SSW of Oslo. Our significantly enlarged data set provides important information for analysing the behaviour of the geomagnetic field and for comparison to the PSV database for lavas of the last 5 Myr and Giant Gaussian Process (GGP; Constable & Parker 1988) model predictions using TK03.GAD (Tauxe & Kent 2004). PSV analyses are represented as VGP dispersion (S) of our data and existing data from the Oslo Graben plotted versus their palaeolatitude, while we also determine the elongation (E) of the directional distributions for comparison to the TK03.GAD field model (Tauxe & Kodama 2009).

The sampled rocks are lower Permian in age, which is a critical time span for Pangaea reconstructions, and until today still much debated (e.g. Domeier *et al.* 2012). The reconstruction of the youngest supercontinent Pangaea that existed from the late Palaeozoic to early Mesozoic was first made by Wegener (1915), who recognized the fit between the present-day Atlantic margins. His reconstruction was further constrained by palaeontological and lithostratigraphical evidence (Köppen & Wegener 1924; Du Toit 1937). The break-up of Pangaea is well known, thanks to the availability of marine magnetic anomalies (Heezen 1960; Dietz 1961), hotspot tracks (Richards *et al.* 1989; Müller *et al.* 1993; Norton 2000) and apparent polar wander paths (APWPs; Creer *et al.* 1954; Besse & Courtillot 2002; Torsvik *et al.* 2012). Pangaea's configuration before its break-up, that commenced when the Atlantic Ocean started opening in the early Jurassic, is less well constrained and solely relies on APWPs.

In classical Pangaea A-type reconstructions, present-day North America is placed north of South America, and Eurasia is placed north of Africa. Early reconstructions derived from the APWPs however, showed an overlap between the Gondwana and Laurussia part of Pangaea in the late Carboniferous and Permian as large as $\sim 15^\circ$ (equivalent to ~ 1650 km). This led Irving (1977) to introduce an alternative configuration, resulting in a controversy that prevails Pangaea reconstructions ever since. Irving's (1977) Pangaea B-type reconstruction places present-day North America west of South America. A large, mainly longitudinal ~ 3500 km shear zone would need to accommodate the necessary right-lateral motion between Gondwana and Laurussia necessary to bring the continents back into their pre-Pangaea break-up position. In addition to palaeomagnetic research aiming at resolving the Pangaea controversy, many studies introducing a variation of geological data types have been performed (Angiolini *et al.* 2007; Schaltegger & Brack 2007; Gutierrez-Alonso *et al.* 2008; Torsvik *et al.* 2008a). The controversy however, is of palaeomagnetic origin.

The data from Permian rocks with well-determined and revised ages provided in this study are relevant to the Pangaea controversy, and we will discuss the implications of our data and ex-

isting data from the Oslo Graben for the position of the northern Pangaea continent (Laurussia). This study is at the moment the most complete one of the Permian Oslo Graben and provides excellent data for both PSV and palaeolatitude analyses of Baltica during the early Permian. Furthermore it aims to update and extend older palaeomagnetic studies of the Oslo Graben (van Everdingen 1960; Storetvedt *et al.* 1978).

2 GEOLOGICAL SETTING AND SAMPLING

The Oslo Graben contains one of the most extensive and best preserved sequences of basaltic lavas in the PCRS. They are associated with the upper Palaeozoic rifting of this area (Fig. 1). The Oslo palaeorift marks the onset of a prolonged period of rifting in NW Europe, caused by extensional faulting and volcanism which lasted throughout the Late Palaeozoic and Mesozoic. The geological and tectono-magmatic development of the Oslo Rift has been studied in detail (e.g. Larsen & Sundvoll 1984; Olausen *et al.* 1994; Heeremans *et al.* 1997; Neumann *et al.* 2002). The Oslo Rift extends from the Southern part of Skagerrak to Western-Central Sweden over a distance of 520 km. The Oslo Graben portion of the rift in southeast Norway is an approximately 220-km-long and 60-km-wide NNE trending on land structure. The tectono-magmatic evolution of the Carboniferous-Permian Oslo Rift system was subdivided in early studies (Sundvoll *et al.* 1992; Heeremans *et al.* 1997) into six stages: (1) the Proto-rift stage (310–300 Ma), (2) the initial rift stage (300–295 Ma), (3) the rift formation stage 1 (290–275 Ma), (4) the rift formation stage 2 (280–275 Ma), (5) the syenitic batholith intrusion stage (270–250 Ma) and (6) the termination stage (250–241 Ma). The Oslo Graben was filled during the Proto-rift stage (1) with sediments and some sill intrusions, and during the initial rift stage (2) by plateau and shield volcanics, which was most extensive in the SW (Vestfold). From the volcanics of the initial rift stage (2) we sampled tholeiitic basalt B₁ northwest of Oslo (Krokskogen; Fig. 1). The main plateau and rift formation took place (3) between 290–275 Ma, when monogenetic fissure eruptions formed extensive rhomb porphyry (RP) lavas that we sampled in both Vestfold (RP series) and Krokskogen (Vestmarka Fm, Kjaglia FM). The number of RP flows strongly increases from north (~ 5 known flows) to south (~ 100 known flows). In the Krokskogen area some 22 flows produced a thickness of ~ 1000 metres in 14 Myr, while in Vestfold we find ~ 3000 metres thickness in 10 Myr. The subsequent initial rift stage (4) is characterised by explosive acidic volcanism and caldera formation. Of phase (4) and of subsequent—mainly intrusive volcanic—phases (5,6) we have not sampled rocks.

The volcanics are traditionally divided into three types after their mineralogy and chemistry: mafic basalts, intermediate rhomb porphyries and felsic trachytes and rhyolites. In the Oslo Graben today the rhomb porphyries are dominant in volume. The distinction between the different rhomb porphyry flows of stage 3 is possible on the basis of variations in shape, size, arrangement and amount of the feldspar phenocrysts in these rocks. It is assumed that the basaltic volcanism started in the south and migrated towards the north, possibly over a period of a few million years (Larsen & Olausen 2005). The rhomb porphyry lava flows vary significantly in thickness, from less than 10 m to close to 160 m. The largest magma volume and the highest extrusion rate lasted from 293 to 283 Ma in the Vestfold graben (on average one flow every 200 kyr and $0.3 \text{ km}^3 \text{ kyr}^{-1}$; Fig. 2). In the Krokskogen area the rate is approximately one flow

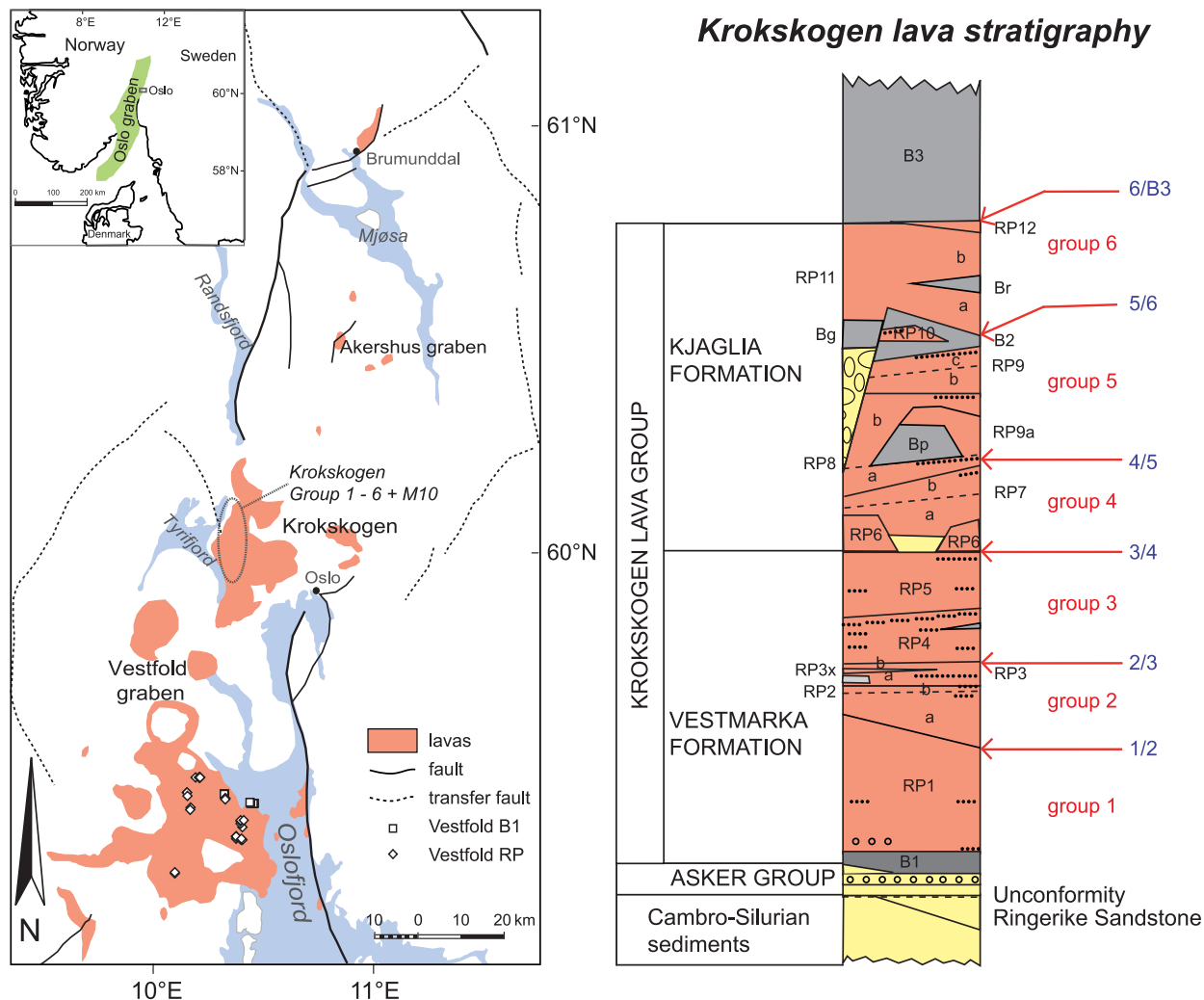


Figure 1. Left-hand panel: simplified geological map of the Oslo Graben area, indicating the location of the lava sequences of Brumunddal, Kroksgogen and Vestfold. Right-hand panel: overview of the lava stratigraphy for the Kroksgogen plateau (after Larsen & Olaussen 2005) which was divided in six groups, the boundaries are indicated by arrows. B indicates basalts, RP are rhomb porphyry lavas. Exact site locations are available as a Google Earth kml file (from C.G.Langereis@uu.nl)

per 800 kyr, while in the Brumunddal area there is no control on the rate.

In the Kroksgogen area, the lowest extrusive igneous unit is a quartz tholeiite basalt (basalt B₁), which is the oldest lava in the sequence (Larsen 1978). This unit was dated by Rb-Sr at 291 ± 8 Ma of (Sundvoll & Larsen 1990), indicating an upper Carboniferous age. The remainder of the sequence consists of rhomb porphyry flows with occasional interbedded sediments and basalts. The assumed age for the earliest lavas (RP₂₊₃) in Vestfold is 294 ± 6 Ma (Sundvoll & Larsen 1990; Neumann *et al.* 2002). The basalts and the lavas are named in stratigraphical order according to their age: B₁ represents the oldest basalt, RP₁ the first oldest lava flow and up to the youngest lava flow RP₁₇. The original lower 12 RP flows (or units) have been expanded—through the discovery of additional intercalated lava flows—into some 22 separate flows, labelled by using suffixes a,b,c,x (Fig. 1). For this study we have sampled the lava flows up to RP₁₂ in Kroksgogen. The individual lava flows cover large areas, therefore they are found at different sites; they also vary significantly in thickness. The number of lava flows is ~50 in Vestfold, ~22 in Kroksgogen and only 4 in Brumunddal.

For the ease of presentation, and to detect a possible time-progressive trend in the palaeomagnetic results of the Kroksgogen Lava Group, we have subdivided the Group into 6 groups (Fig. 1), forming the older Vestmarka formation (groups 1–3) and the younger Kjaglia formation (groups 4–6). Similarly, we have divided the Vestfold lavas into a lower mainly basaltic B1 Formation and a younger (overlying) rhomb porphyry RP lava formation.

The lavas found in the Oslo Graben form the most extensive suite of primitive basalts in the large European Permo-Carboniferous rift system (Neumann *et al.* 2002). The first palaeomagnetic results of the Oslo Graben lavas were provided by Everdingen (1960). His results are frequently used in the palaeomagnetic discussions on the Permian pole positions of the Baltica part of Laurussia. Everdingen (1960) sampled the following Permian rock units from Kroksgogen and Vestfold: basalts (B₁–B₄), rhomb porphyries (RP₁–RP₁₇) and syenite-porphyrines (SP₁–SP₃). Storetvedt *et al.* (1978) extended van Everdingen's (1960) study by sampling 23 new sites.

Earlier work was mostly done by alternating field demagnetization in a limited number of steps. Our goal was to verify the stability of the magnetization, and its origin, using modern palaeomagnetic

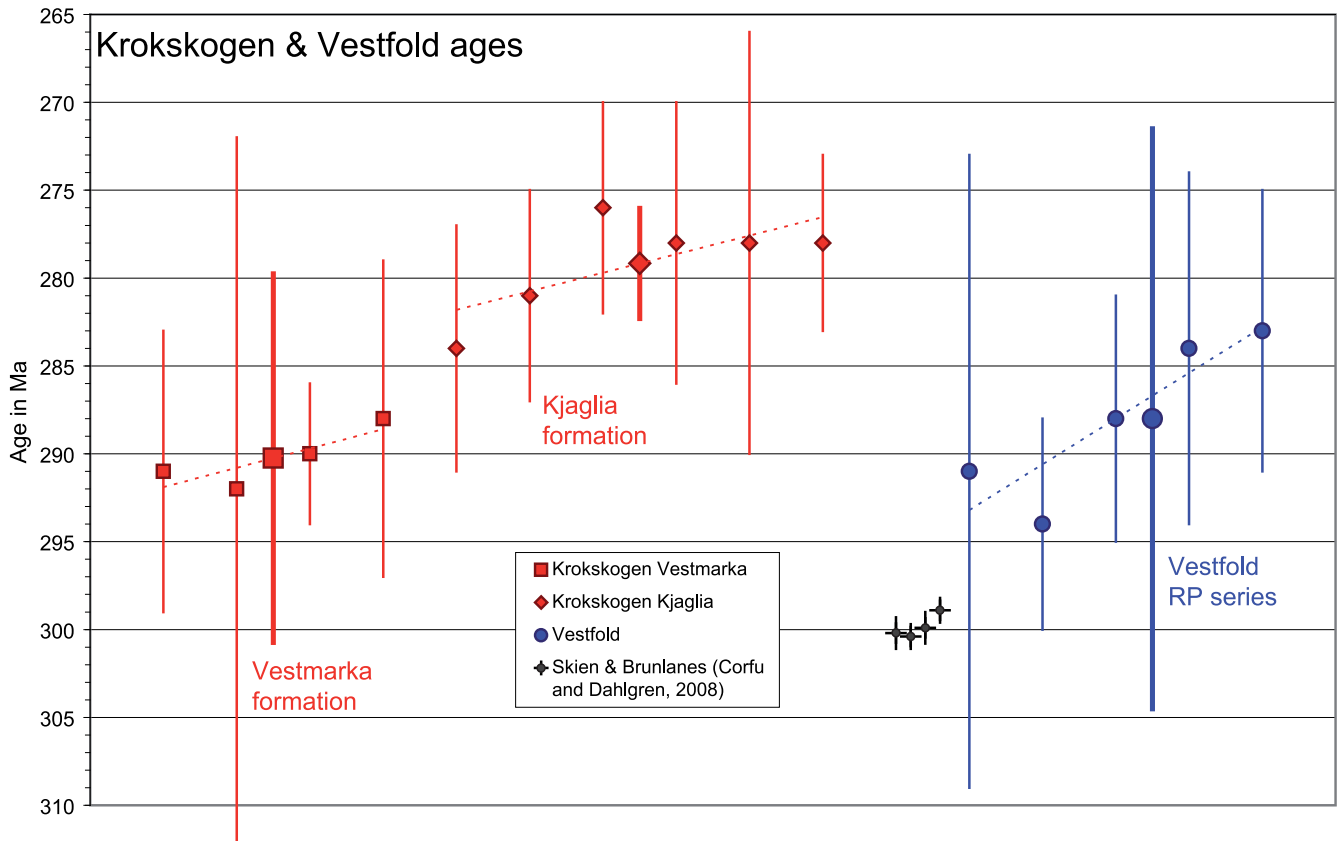


Figure 2. Ages (Rb–Sr and $^{40}\text{Ar}/^{39}\text{Ar}$) of the Krokskogen and Vestfold plateaus from Sundvoll & Larsen (1990). Indicated are the Vestmarka and Kjaglia formations of Krokskogen; in Vestfold ages refer only to the RP series. The Skien and Brunlanes basalts are the oldest known volcanics in Vestfold. The Skien and Brunlanes U–Pb ages are according to Corfu & Dahlgren (2008). There is an increasing trend in all three groups, indicated by the dotted linear regression lines. The age of the Vestfold B series must be younger than the Skien and Brunlanes basalts, and older than the (average) age of the RP series.

and rock magnetic techniques. A reassessment is warranted because the Oslo Graben volcanics provide an important constraint on the Permian Eurasian APWP, and have implications for the Pangaea A versus Pangaea B controversy. We also use revised and better constrained ages of the Oslo lava flows, based on the Rb–Sr and $^{40}\text{Ar}/^{39}\text{Ar}$ measurements of Sundvoll & Larsen (1990). We have divided the Krokskogen lava formation in two age ranges (Fig. 2), one for the Vestmarka formation (290.3 ± 10.5 Ma) and one for the Kjaglia formation (279.2 ± 3.1 Ma). The Vestfold volcanics ages range 288.0 ± 16.5 Ma and ages have large errors (Fig. 2), but reported ages apply only to the RP series (Sundvoll & Larsen 1990). The underlying basaltic B1 series must be older than the RP series, but younger than the oldest lavas in Vestfold—the Skien and Brunlanes basalts—which have been accurately dated by U–Pb at around 300 ± 1 Ma (Corfu & Dahlgren 2008). We therefore assign an age range to the B1 series between 300 and 288 Ma, and for the RP series the published age of 288.0 ± 16.5 Ma. Our best estimate of the age range of the entire Krokskogen group is then approximately 284 ± 8 Ma, and of the entire Vestfold group approximately 292 ± 8 Ma (Fig. 2).

For this study, a large number of lava flows was sampled from both the Krokskogen and Vestfold lava plateaus (Fig. 1). A total of 944 oriented cores were taken, partly in the Krokskogen area (NW of Oslo), and partly in the Vestfold area (on the western side of the Oslo fjord; Fig. 1). The cores were taken using a gasoline powered drill and oriented with both a magnetic and sun compass. We collected at least 8 oriented cores from each site (Table 1). In Krokskogen we

sampled 57 sites in total: 51 sites (391 cores) in basalts and rhomb porphyries and four sites (36 cores) in red sandstones; one site in sediments below basalt B₁ gave no results, one site in a syenite was not used (see Table S1). In Vestfold, we sampled 52 sites (346 cores) in basalts and rhomb porphyries; three sites gave no results. In the Brumunddal area we sampled only red beds (207 cores) which yielded no interpretable results. Hence, in total we report the results from 104 sites. For all sites, we measured the strike and dip, if possible, on the contacts between lava flows, on planes parallel to these contacts, or on bedding planes of intercalated sediments when available. If direct measurements of strike and dip were not possible, the bedding plane was reconstructed from the geological maps, and by using satellite imagery from Google Earth. In some cases however, the bedding plane was unclear or ambiguous.

3 ROCK MAGNETIC AND PALAEOMAGNETIC ANALYSES

3.1 Rock magnetic analyses

3.1.1 Curie balance

Thermomagnetic runs were measured (21 representative experiments for Krokskogen and 10 for Vestfold) in air with a modified horizontal translation type Curie balance (Mullender *et al.* 1993; sensitivity $\sim 5 \times 10^{-9}$ Am²). Approximately 30 mg of powdered rock was put into a quartz glass sample holder and held in place by

Table 1. Summary of palaeomagnetic results (this study and literature data) for the Oslo Graben. N , number of samples used in the statistics; S , VGP scatter with 95 per cent bootstrap bounds (S_l , S_u); Dec, declination; Inc, inclination; k , estimated Fischer precision parameter; α_{95} , confidence circle at the 95 per cent level; ΔD_x , declination error; ΔI_x , inclination error derived from A_{95} according to Butler (1992); λ , palaeolatitude; K , precision parameter and A_{95} , cone of confidence determined from the mean VGP direction; P_{lat} , latitude of pole position; P_{long} , longitude of pole position; E , elongation with 95 per cent bootstrap error bounds (E_l , E_u).

Area	N	S_l	S	S_u	Dec	Inc	k	α_{95}	ΔD_x	ΔI_x	λ	P_{lat}	P_{long}	K	A_{95}	E_l	E	E_u
Krokskogen–Vestmarka fm.	26	9.4	11.6	13.7	205.7	-40.1	47.4	4.2	4.9	6.2	22.9	49.0	153.1	41.0	4.5	1.71	2.53	5.05
<i>ctmd</i> : $g = 8.6 > g_c = 5.5$ (negative)	<i>no tc</i>	8.7	10.6	12.8	194.7	-42.3	67.9	3.5	4.1	4.9	24.5			58.5	3.7	1.16	1.78	4.50
Krokskogen–Kjaglia fm.	29	7.3	8.5	9.7	209.3	-39.9	93.5	2.8	3.0	3.0	22.7	47.6	148.3	92.0	2.8	1.12	1.61	3.59
<i>ctmd</i> : $g = 8.4 > g_c = 4.1$ (negative)	<i>no tc</i>	7.8	9.0	10.4	199.7	-44.3	80.6	3.0	3.3	3.8	26.0			81.6	3.0	1.17	1.98	4.55
Vestfold–B1 series	18	6.7	9.2	11.2	202.5	-30.9	54.6	4.7	4.1	6.3	16.7	44.4	159.7	78.0	3.9	1.45	2.53	7.78
<i>ctmd</i> : $g = 18.8 > g_c = 6.7$ (negative)	<i>no tc</i>	5.6	7.9	9.8	205.9	-12.4	55.6	4.7	3.4	6.5	6.3			105.3	3.4	1.42	2.68	8.13
Vestfold–RP series	31	8.1	10.8	13.7	198.8	-38.0	41.3	4.1	3.8	5.0	21.3	50.1	162.1	54.8	3.5	1.41	2.55	7.48
<i>ctmd</i> : $g = 15.1 > g_c = 6.0$ (negative)	<i>no tc</i>	8.0	11.0	13.9	205.1	-23.9	30.7	4.7	3.6	6.2	12.5			54.7	3.5	2.13	4.61	15.68
Krokskogen	55	9.3	10.7	12.3	207.6	-40.0	64.1	2.4	2.8	3.5	22.8	48.3	150.5	57.5	2.6	1.24	1.80	3.11
<i>ctmd</i> : $g = 8.4 > g_c = 3.4$ (negative)	<i>no tc</i>	8.6	10.0	11.5	197.3	-43.4	72.0	2.3	2.6	3.1	25.3			65.9	2.4	1.08	1.17	2.16
Vestfold	49	8.7	10.7	12.7	200.3	-35.4	42.1	3.2	2.9	4.0	19.5	48.0	161.1	58.2	2.7	1.22	1.98	4.17
<i>ctmd</i> : $g = 17.3 > g_c = 5.2$ (negative)	<i>no tc</i>	8.3	10.4	12.4	205.4	-19.6	31.8	3.7	2.7	4.8	9.8			61.2	2.6	1.72	3.31	7.16
Krokskogen and Vestfold this study	104	10.1	11.3	12.5	204.0	-37.9	46.9	2.0	2.1	2.8	21.3	48.3	155.5	52.2	1.9	1.07	1.26	1.98
<i>ctmd</i> : $g = 5.8 > g_c = 3.7$ (negative)	<i>no tc</i>	12.1	13.3	14.5	201.6	-32.4	22.4	3.0	2.4	3.6	17.6			37.7	4.6	2.86	4.13	6.30
Krokskogen and Vestfold, van Everdingen (1960)	27	6.0	7.5	9.2	203.9	-35.6	88.1	3.0	2.7	3.9	19.7	47.0	157.0	116.5	2.6	1.28	2.31	5.34
<i>ctmd</i> : $g = 1.9 < g_c = 4.6$ (Class. A)	<i>no tc</i>	7.6	9.3	11.4	204.9	-32.9	56.0	3.7	3.4	5.0	18.0			76.5	3.2	1.41	2.23	4.84
Lunner dykes, Dominguez et al. (2011)	38	6.1	8.5	11.3	198.2	-32.9	90.2	2.5	2.7	3.3	23.2	51.0	163.0	89.0	2.5	1.64	2.75	5.71

quartz wool. Temperatures were increased to a maximum, of 700 °C (heating and cooling rates 10 °C min⁻¹). At selected temperatures during heating, the temperature was lowered by 100 °C before heating to more elevated temperatures to check for chemical alterations during the experiment. Curie temperatures were determined with the two-tangent method (Grommé *et al.* 1969).

At a first glance, the samples generate different results for the measurements on the Curie balance (Fig. 3). The first difference lies in the magnetization of the cooling curve which is higher than the warming curve for, for example, the HO39_6 and HO43_8 samples (Fig. 3b). This is due to haematite (with a Néel temperature close to 680 °C) which was not saturated by the cycling field of 150–300 mT (de Boer & Dekkers 2001). The results for the samples HO24_11 and HO29_1 (Figs 3a and b) show typical curves for magnetite (Curie point 580 °C). Samples HO4.1 and HO15.7 show a Curie temperature of 580 °C and a Néel temperature of 680 °C pointing to the presence of both magnetite and haematite minerals.

3.1.2 Acquisition curves of isothermal remanent magnetization (IRM)

To further characterize the NRM of the samples, the magnetic mineralogy was assessed by carrying out rock magnetic measurements. A MicroMag Model 2900 alternating gradient magnetometer was used, equipped with a 2 Tesla magnet—but effectively 1.6 Tesla because of partial saturation of the pole shoes—(Princeton Measurements Corporation, noise level 2×10^{-9} Am²). Successively, hysteresis loops and IRM acquisition curves were measured, all at room temperature.

We carried out the IRM measurements on 15 samples in order to identify the different IRM components using the fitting method of Kruijer *et al.* (2001). The IRM acquisition curves contain 200 data points; examples of representative samples are given with the fitted IRM components (Fig. 4). The IRM acquisition curves could be interpreted with two magnetic components. A third, small component with a low intensity and low coercivity was usually observed, as a result of slightly skewed-to-left data (Heslop *et al.* 2004). This component is not assigned a physical meaning, because it is a consequence of the method to fit symmetric distributions. The two magnetic components invariably present in the samples are (Fig. 4): a relatively weak low-coercivity component with $B_{1/2}$ values ranging 30–60 mT which we interpret as magnetite, and a relatively strong high-coercivity component with values ranging 500–800 mT indicative of hematite. Occasionally, high-coercivity values of ~200 mT point to oxidized magnetite (maghemite).

3.2 Palaeomagnetic analyses

The characteristic remanent magnetizations (ChRM) of the lava specimens was determined by applying thermal (TH) demagnetization, conducted with steps of 100 to 300 °C or 400 °C; for higher temperatures (max. 700 °C), the intervals were reduced to 50 °C and finally down to 10 °C steps, to permit a more detailed study of the NRM demagnetization. The TH demagnetization was measured on a horizontal 2G Enterprises DC-SQUID cryogenic magnetometer (noise level 3×10^{-12} Am²). Some of the specimens were also demagnetized using alternating field (AF) demagnetization with steps of 3–20 to 120 mT with an in-house developed robot assisted and fully automated 2G DC-SQUID cryogenic magnetometer (noise level 10^{-12} Am²). The presence of a high coercivity component (hematite) prevented full demagnetization using AF

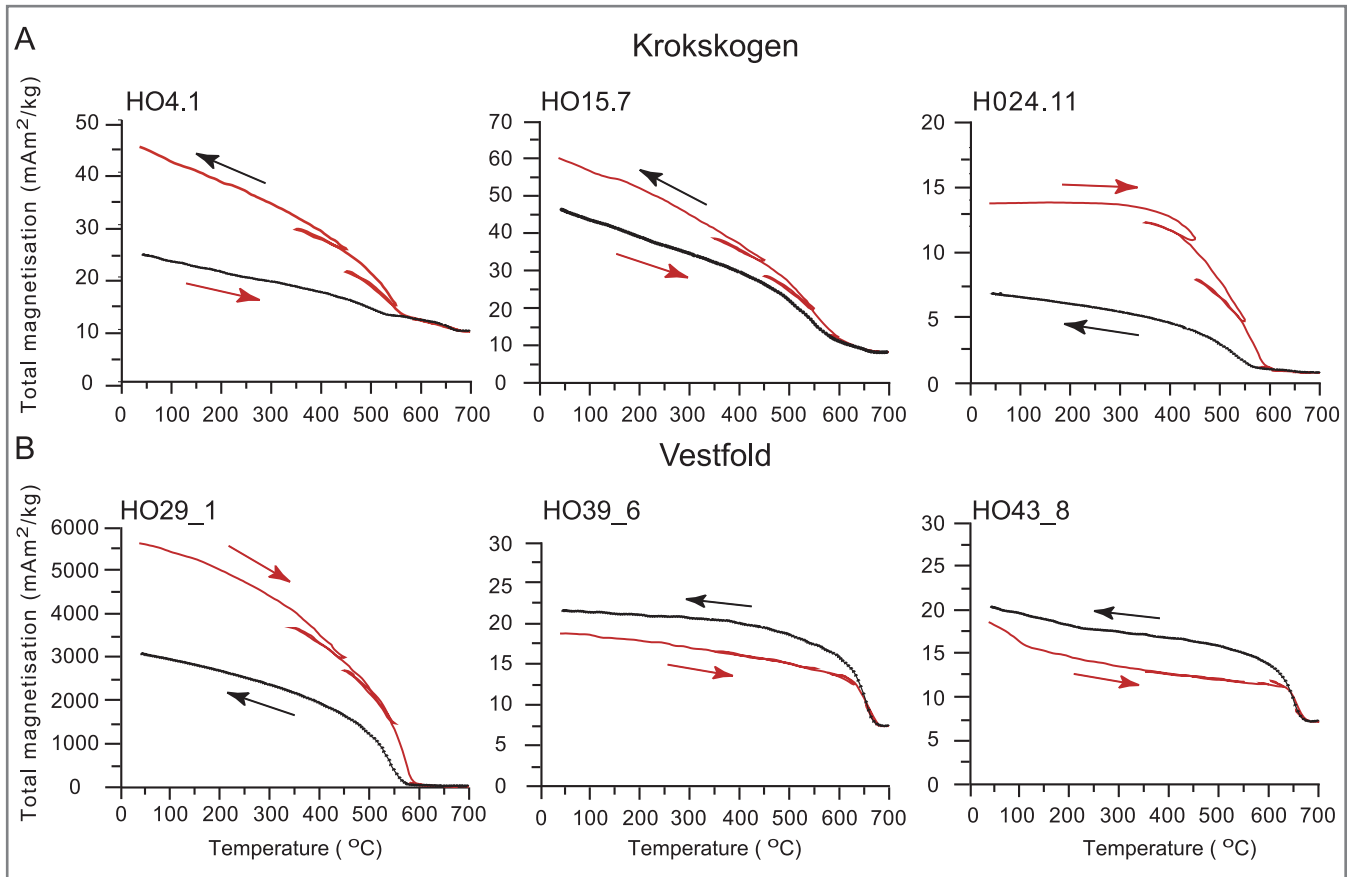


Figure 3. Representative thermomagnetic curves measured on a Curie balance (Mullender *et al.* 1993) for characteristic samples from the Krokskogen and Vestfold plateaus. Arrows indicate heating (red) and cooling (black) curves. The results show both (Ti-poor) magnetite and hematite as main carriers of the NRM.

demagnetization techniques, as is evident from the IRM and Curie balance experiments. Therefore, the samples were further demagnetized using only thermal demagnetization.

Demagnetization of the NRM is displayed in orthogonal vector diagrams (Zijderveld 1967); representative examples are shown in Fig. 5. Magnetization components were determined using principal component analysis (Kirschvink 1980) typically on five to ten successive temperature steps. The maximum unblocking temperature ranges 560–680 °C. We conclude that the magnetic carriers in these samples vary from magnetite/maghemite to hematite, in line with the rock magnetic results, which agree with the behaviour of normalized thermal decay curves of the NRM (Fig. 5).

A component close to the present day GAD field is present in nearly all samples, which was typically removed after heating to 200 °C. In many samples there is an inflexion around 350 °C, pointing to inversion of maghemite (Dankers 1978). Usually, there is a magnetite component, as can be seen from the thermal decay curves (Fig. 5). At the highest temperatures a component was usually isolated between 600 and 680 °C, therefore residing in hematite. These results lead us to conclude that these samples usually carry two high-temperature magnetization components: one low coercivity component carried by magnetite/maghemite and a second high coercivity component carried by hematite (Figs 4 and 5). Both components show identical directions. Occasionally, the NRM could not be completely removed, resulting in erratic behaviour of the NRM at temperatures above 500 °C, probably because of the growth of new magnetic minerals during thermal demagnetization. Fig. 6 shows

examples of the ChRM directions from representative sites in equal area projections. Site means and VGP means were calculated using Fisher statistics (Fisher 1953). The error in declination (ΔD_x) and the error in inclination (ΔI_x) were calculated following Butler (1992). We favour this approach because it describes the directional distributions more realistically: they become increasingly elongated with lower latitudes (Creer *et al.* 1959; Tauxe & Kent 2004; Tauxe *et al.* 2008; Deenen *et al.* 2011). The results of all individual sites are given in Table S1, while the results per group and per area are given in Table 1. Microscopic analysis of the Oslo Graben volcanics (van Everdingen 1960) showed that many samples from the study by van Everdingen (1960) showed only hematite, but for example the basalt formation B1 (Vestfold) shows magnetite and some alteration of maghemite. The rhomb porphyry lavas usually contain evidence for hematite or magnetite and martitized maghemite. These observations are in agreement with the rock magnetic and palaeomagnetic behaviour of our samples. Unfortunately, the samples are therefore not suitable for absolute palaeointensity determination.

4 PALAEOMAGNETIC RESULTS AND DISCUSSION

4.1 Palaeomagnetic results

From the ChRM directions, site means as well as VGPs and their means were calculated (Figs 6 and 7). To determine whether two distributions share a common true mean direction (ctmd) we used

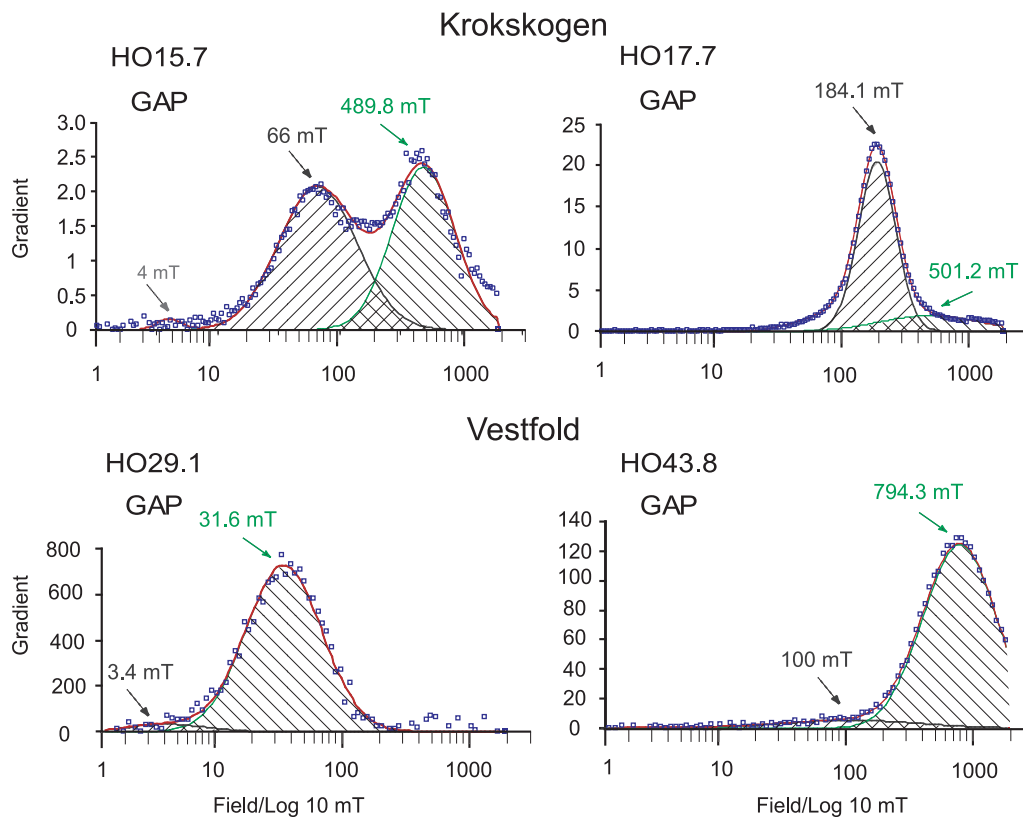


Figure 4. Representative examples of IRM component analysis (Kruiver *et al.* 2001) for samples from the Krokkskogen and Vestfold plateaus. Squares are measured data points. The various components are marked with different lines: component 1 (green line) has a low coercivity and component 2 (grey dashed line) has a high coercivity; the gradient acquisition plots (GAP) are shown in different hatches for each component. Values of $B_{1/2}$ are displayed in each panel together with their dispersion parameter (DP). The saturation isothermal remanent magnetization (SIRM) is given in $A m^{-1}$. Krokkskogen: HO 15 is from RP 2a, HO 17 from RP 1 (see Fig. 1); Vestfold: HO 29 is from the B1 series, HO 43 from RP 5 (see also Table S1).

the reversal test developed by (McFadden & McElhinny 1990). We have modified the software to accommodate the test also to distributions with the same polarity. We use Monte Carlo simulation, thereby effectively applying the (Watson 1983) V_w statistic test. We determine γ , the angle between the means, and γ_c , the critical angle in the test. If $\gamma < \gamma_c$ the test is positive and the distributions share a common true mean direction. The quality of the test is expressed as A, B, C or indeterminate, depending on the value of γ_c (McFadden & McElhinny 1990).

Of the 55 sites in Krokkskogen (26 in the Vestmarka Fm., 29 in the Kjagla Fm.), one site gave no results (HO 20, intercalated sediments; see Table S1). In Vestfold, of the 20 sites from the B1 group one site (MO 42) gave no results. One site (MO 45) has very low k (10.3) and high α_{95} (24.6) and was therefore rejected. Of the 32 sites from the RP group only one site (MO 60) gave no sensible results.

In general the directions per site/flow cluster well, having k values typically ranging 35–400, while ca. 50 per cent of all sites has k values higher than 100 (Table S1). Nevertheless, k values are quite low when compared to ‘regular’ lava flows that cool in a short time and record spot readings of the geomagnetic field. This is likely due to the nature of the rhomb porphyry lavas of which the cooling rate is unknown but likely longer than in ‘regular’ tholeiitic flows, considering their thickness and their crystallinity containing (5–20 per cent) large (5–20 mm) feldspar phenocrysts. Hence, we probably have sampled both relatively quickly cooled lavas giving high k values and tight clustering, as well as relatively slowly cooled

lavas that recorded some secular variation and thus having lower k values (Fig. 6).

We have first averaged the directions from Krokkskogen in six groups (Fig. 7), to see if we could detect any time progressive or systematic behaviour. This was not apparent, however, the groups have means that share either no ctmd (e.g. groups 1, 2, 3 do not share a ctmd with each other) or means that do share a ctmd (e.g. groups 4, 5, 6 share a ctmd with classification B). Upon tilt correction the number of ctmd’s between groups improves slightly. We have then combined the groups into two formations, the Vestmarka (groups 1, 2, 3) and Kjagla (groups 4, 5, 6) formations (Table 1). The two formations share a ctmd (classification A), both before and after tilt correction. In Vestfold, we have averaged two groups/formations (the B1 and RP series; Table 1). However, the two groups do not share a ctmd, both before and after tilt correction.

For all four formations we have applied the fold test (Fig. 8). In all cases, the fold test is inconclusive and not statistically significant. This is evidently caused by very similar strikes and dips of the bedding. Additionally, the measured bedding tilts are of the same order as the observed secular variation. Nevertheless, in all cases, the directions before and after tilt correction never share a ctmd (Table 1).

We combined all directions from the two areas, Krokkskogen and Vestfold respectively, to allow a check of the results with the earlier study of van Everdingen (1960) who also combined all sites from the two areas (Table 1). Results from both studies share a ctmd after tilt correction ($\gamma = 2.3^\circ < \gamma_c = 3.6^\circ$, classification A). However,

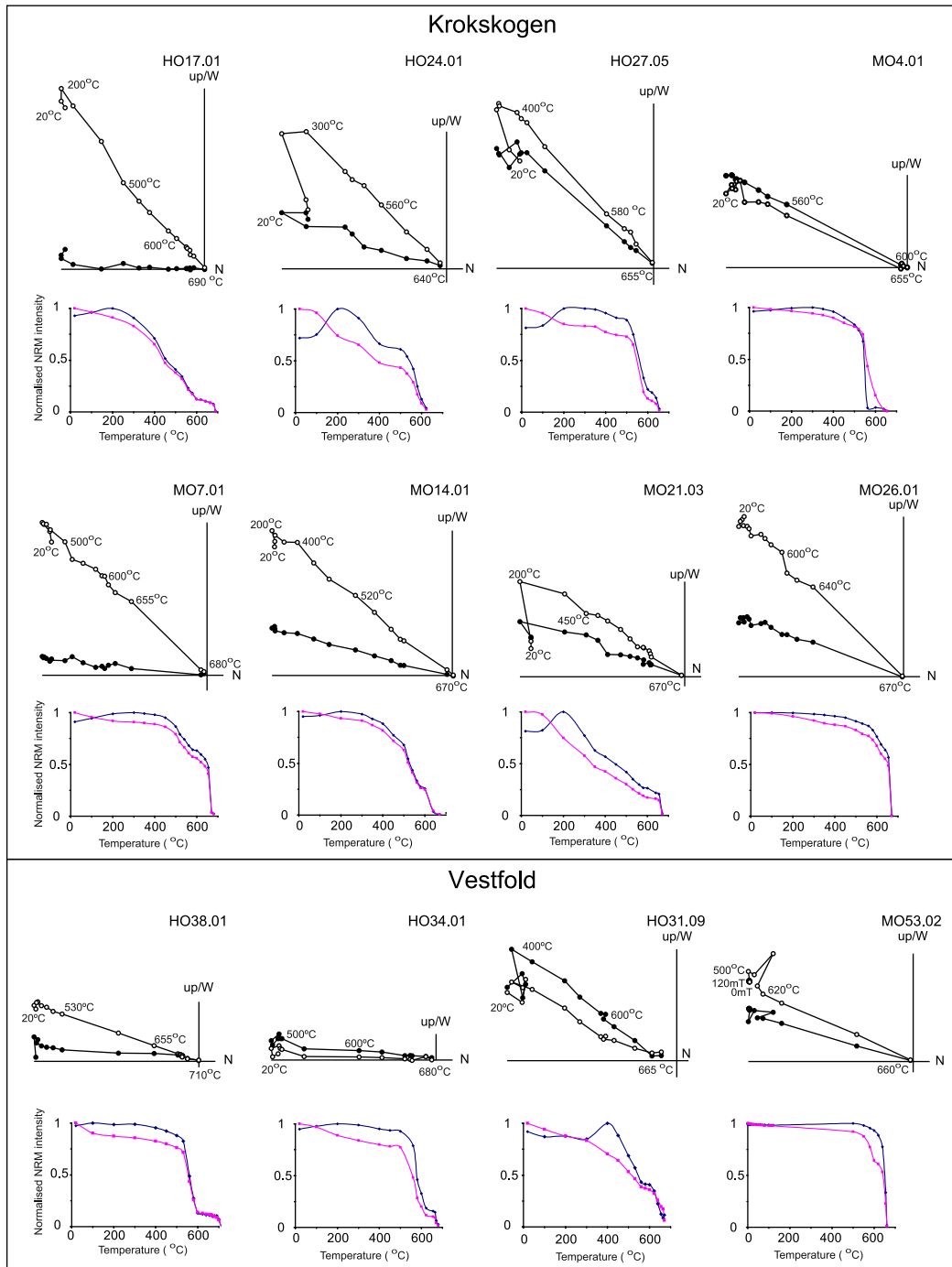


Figure 5. Orthogonal vector diagrams (Zijderveld 1967) of typical demagnetization behaviour (in tilt corrected coordinates) and corresponding decay curves during thermal treatment. Closed (open) symbols denote projections on the horizontal (vertical) plane. Temperatures are indicated in degrees Celsius for key demagnetization steps. The dark blue lines represent decay of the magnetization with respect to the origin; pink lines represent decay along the difference vector sum.

we now have a better age control, and present our results as different age groups.

We have plotted all our poles for the four different formations, the two areas and for the entire Oslo Graben in Fig. 9(b). The mean palaeomagnetic pole for the Vestfold area is in better agreement with the latest pole path of Torsvik *et al.* (2012) than with the earlier version (Torsvik *et al.* 2008b), which did not in-

clude a uniform flattening factor of 0.6 for detrital sedimentary poles. The mean palaeomagnetic pole for the Vestfold area furthermore agrees well with the result of Dominguez *et al.* (2011). The Kroksgogen pole is situated to the west of the pole path, caused by the slightly more clockwise declination of the Kroksgogen area (208°) compared to the Vestfold (200°) and Lunner Dykes (198°) declinations.

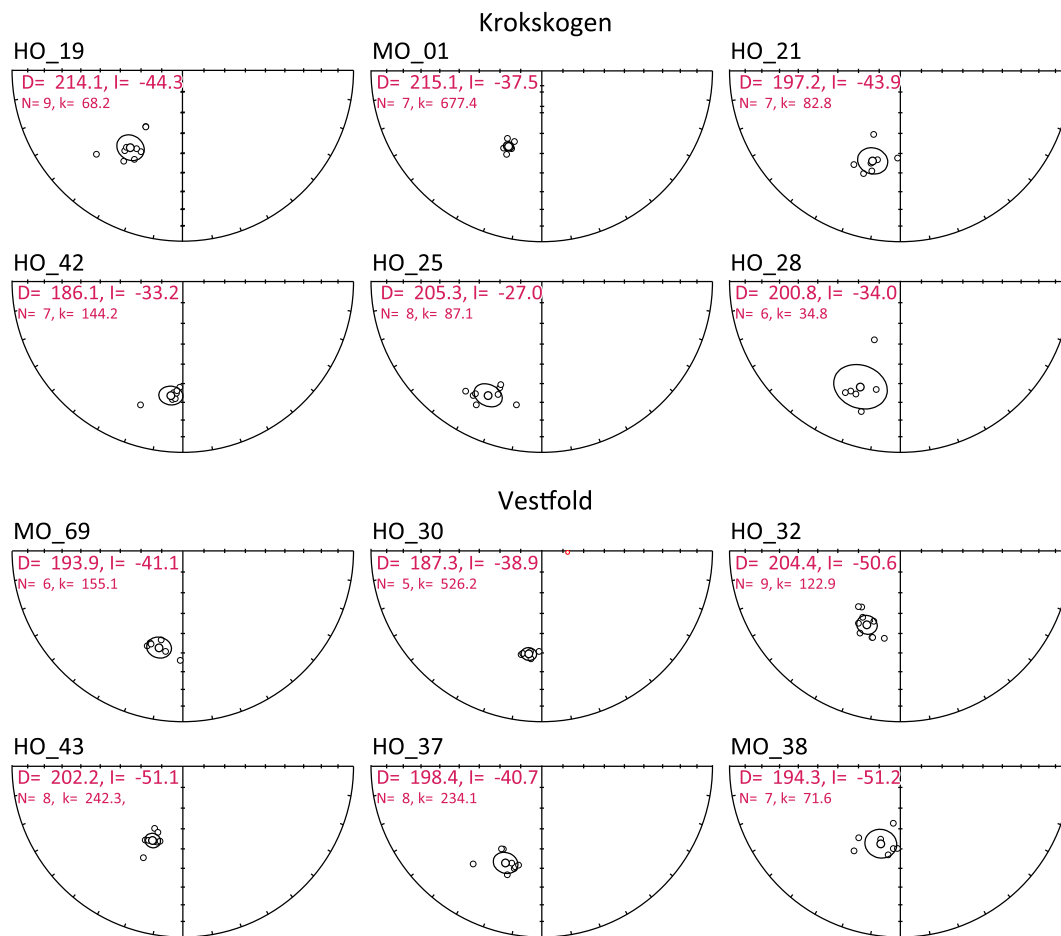


Figure 6. Equal area plots of the observed directions for selected sites. Open/closed symbols indicate negative/positive inclinations. All data are in the supporting information. D , declination; I , inclination.

4.2 Palaeomagnetic discussion and implications for Pangaea reconstructions

The ctmd between our overall mean of the four formations and the study by van Everdingen (1960) implicates that the AF demagnetization technique used half a century ago successfully recovered the mean direction of the Oslo Graben volcanics from the Krokskogen and Vestfold lava plateaus. The earlier results are therefore confirmed by our study that was carried out with modern TH and AF demagnetization techniques and comprises a larger number of successful sites (104 versus 27). Our re-analysis of age data (Fig. 2) from the Oslo Graben volcanics allowed a subdivision of the data in two different areas (that do not share a ctmd) and four formations that show a clear northward palaeolatitude trend with decreasing ages. The trend is similar to the northward trend calculated from the APWPs (Torsvik *et al.* 2008b, 2012; Fig. 9a). Our data display palaeolatitudes that are consistently higher than the palaeolatitudes calculated from the Torsvik *et al.* (2008b) APWP. A comparison to the latest and updated pole path of Torsvik *et al.* (2012) however, leads to palaeolatitudes for the Oslo region that are statistically indistinguishable from our data. We compare Laurussia reconstructions based on our Vestfold (292 ± 8 Ma) and Krokskogen (284 ± 8 Ma) poles with the recommended spline path for Laurussia (Torsvik *et al.* 2012) in Figs 10(a) and (b). The Vestfold pole results in an overall more northerly position of Laurussia with respect to the position calculated from the spline path (Fig. 10a), whereas

the westward location of our Krokskogen pole with respect to the global pole (see Fig. 9b) clearly results in a counterclockwise rotation of our reconstruction with respect to the reconstruction based on the spline path (Fig. 10b). The recent study by Dominguez *et al.* (2011) on younger dykes from northern part of the Oslo Graben (~ 270 Ma) was incorporated in the latest pole path and is in good agreement with Torsvik *et al.* (2012). Compared to our data, it does not show an evident ongoing northward motion of the Oslo Graben region throughout the Permian. This can be ascribed to the error in palaeolatitude which leaves room for different fits through the data.

Before discussing the data presented in this study in the light of the Pangaea controversy, its origin and developments will be discussed below. The first Pangaea B reconstruction by Irving (1977; see Introduction) was quickly followed by a publication by Arthaud & Matte (1977). They presented evidence for the existence of a right-lateral shear zone displacing Laurussia and Gondwana by linking a series of rifts that extended from the Urals to the Appalachians. Proposed timing of a transition from Pangaea B to Pangaea A has varied widely throughout the years, from Permian and Triassic (Morel & Irving 1981), Triassic (Torq *et al.* 1997) to Permian (Muttoni *et al.* 2003, 2009). Interestingly, Torsvik *et al.* (2012) mention that the initial stages of Pangaea formation are unclear as a result of data paucity in the concerned time window and show an early Carboniferous (~ 350 Ma) Pangaea B configuration. This configuration supposedly transformed into Pangaea A by the late Carboniferous, as was also suggested by Domeier *et al.*

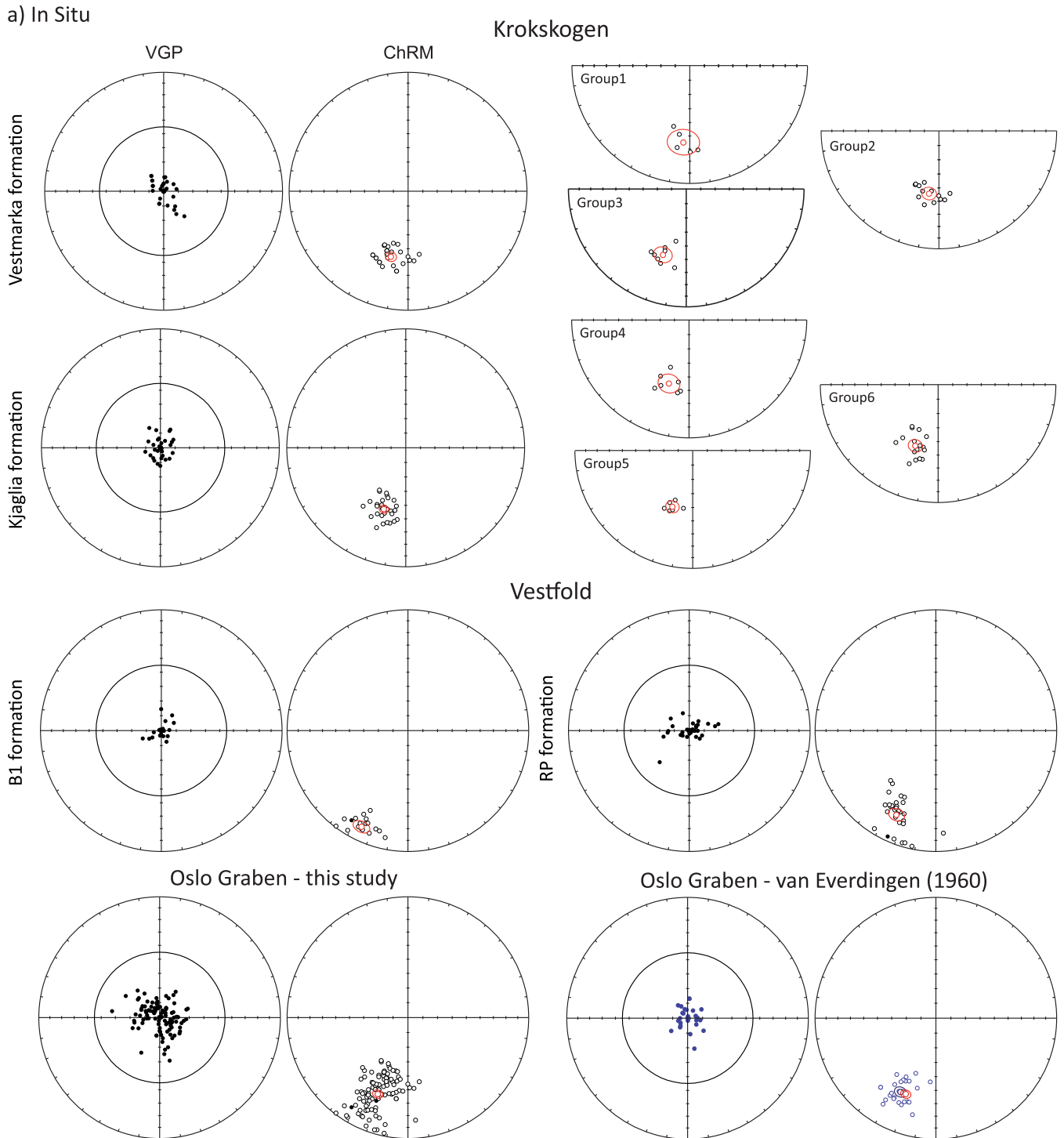


Figure 7. Equal area plots in situ (a) and tilt corrected (b) of the observed directions and their mean (large red symbols, with the α_{95} circle) together with their corresponding VGP's shown with respect to their mean for the Krokskogen and Vestfold groups. The overall mean for the Oslo Graben (Krokskogen plus Vestfold) is also shown (in red) for comparison with the van Everdingen (1960) study (blue symbols). Open/closed symbols indicate negative/positive inclinations. Statistics of the data are listed in Table 1.

(2012). The Gondwana reconstructions by Muttoni *et al.* (2003, 2009, 2013) that point to Pangaea B rely on palaeomagnetic data from North Africa (Sudan, $N = 1$; Morocco, $N = 2$) and Adria ($N = 7$), a promontory of the African plate. Their mean 280 Ma pole for Gondwana derived from these data results in a significantly more northern position of Gondwana compared to Torsvik *et al.*'s (2012) 280 Ma pole ($N = 56$) from the global APWP (GAPWaP) which also

includes the three North African poles selected by Muttoni *et al.* (2013), therefore resulting in an overlap of Gondwana and Laurussia (see Figs 10b and c for reconstructions). Even though the Sudanese, Moroccan and Adrian poles are derived from magmatic rocks and have therefore not been affected by inclination shallowing, the choice of using these poles for Gondwana reconstructions is questioned by several authors (see Domeier *et al.* 2012). One argument

b) Tilt corrected

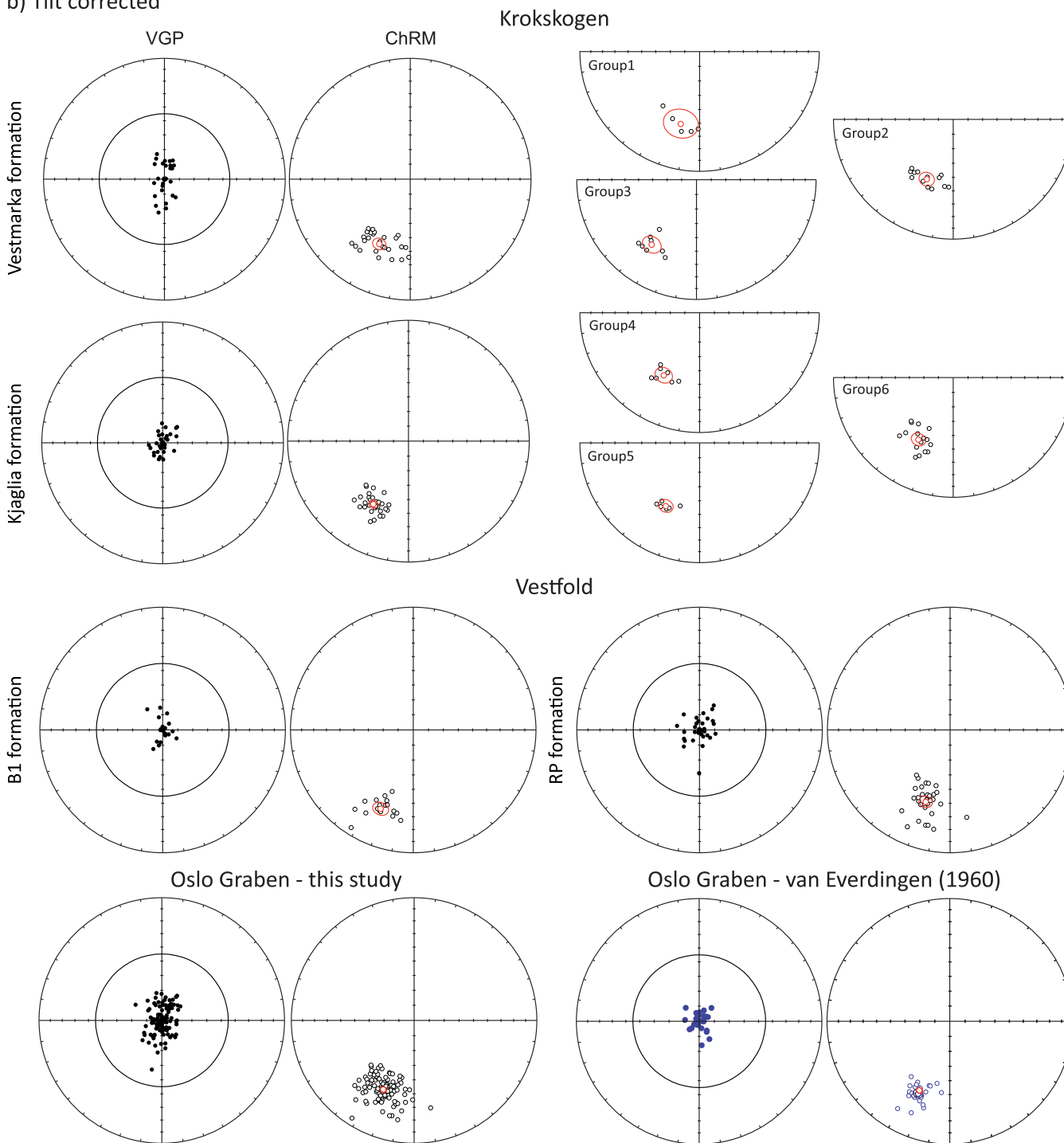


Figure 7. (Continued).

is based on the publication year of the individual poles and their associated errors, since eight of the 10 poles were published between 1969 and 1984 (see references in Muttoni *et al.* 2013). The intrusive nature of many sites selected by Muttoni *et al.* (2013) raises questions about the determination of the palaeohorizontal as well. Revisiting and resampling the early Permian (Adria and Africa) sites included in Muttoni *et al.*'s (2013) compilation would likely reduce the (often large) error of the individual data sets which are based on fewer flows than is presently the norm. In addition, the

poles from Adria may need correction because of a possible rotation of Adria with respect to Africa since 20 Ma (Van Hinsbergen *et al.* 2014).

From the palaeomagnetic community, various approaches aimed at resolving the problem of the overlapping northern and southern continents without involving a Pangaea B configuration. Possible solutions came from applying a series of quality criteria to European poles (Van der Voo & Torsvik 2004), by evaluating the effect of inclination shallowing (Rochette & Vandamme 2001) and

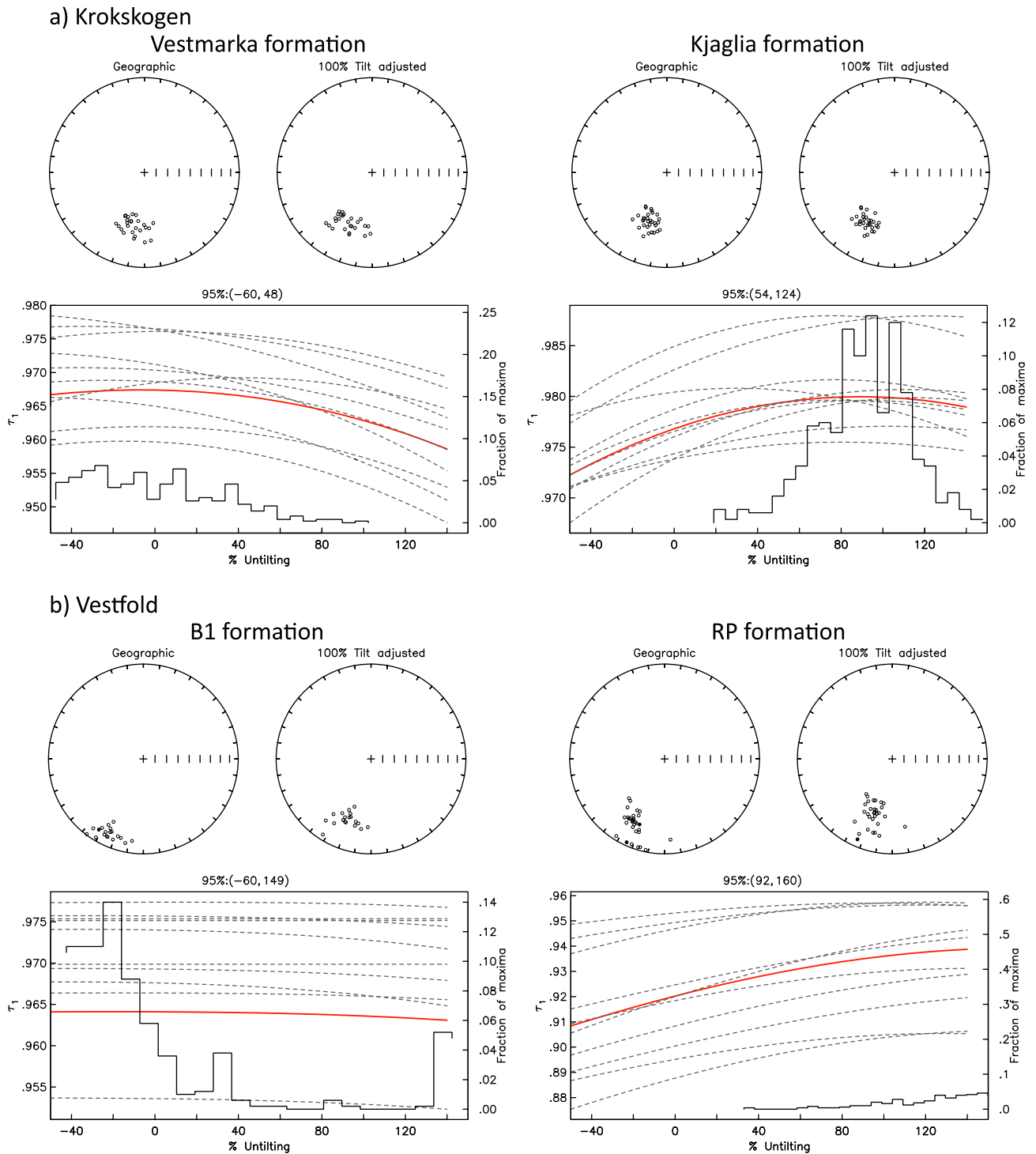


Figure 8. Fold test (Tauxe & Watson 1994) for the means of all the individual samples for the Krokstogen and Vestfold plateau. Although 100 per cent untilting falls within the bootstrap error limits as given above each panel, the fold test is clearly not significant. This is caused by the generally small dips of the bedding, the largely similar strikes per area; differences are of the same order as the recorded secular variation.

by introducing an octupolar contribution to the Earth’s magnetic field (Kent & Smethurst 1998; Van der Voo & Torsvik 2001). A review by Domeier *et al.* (2012) discusses the development of Pangaea reconstructions over decades and the various approaches that have been presented to solve the debate. As we stated above, the problem is of a purely palaeomagnetic origin and therefore Domeier *et al.* (2012) extensively discuss the effect of all palaeomagnetic bi-

ases that may influence the reconstructions (e.g. non-dipole fields, inclination shallowing, age errors and the effect of (partial) remagnetizations) and present new reconstructions based on the latest updated GAPWaP of Torsvik *et al.* (2012) that introduces a flattening factor of 0.6 to detrital sediment data sets uncorrected for inclination shallowing. Their reconstructions based on a combination of these revised palaeomagnetic data with newly available Euler poles

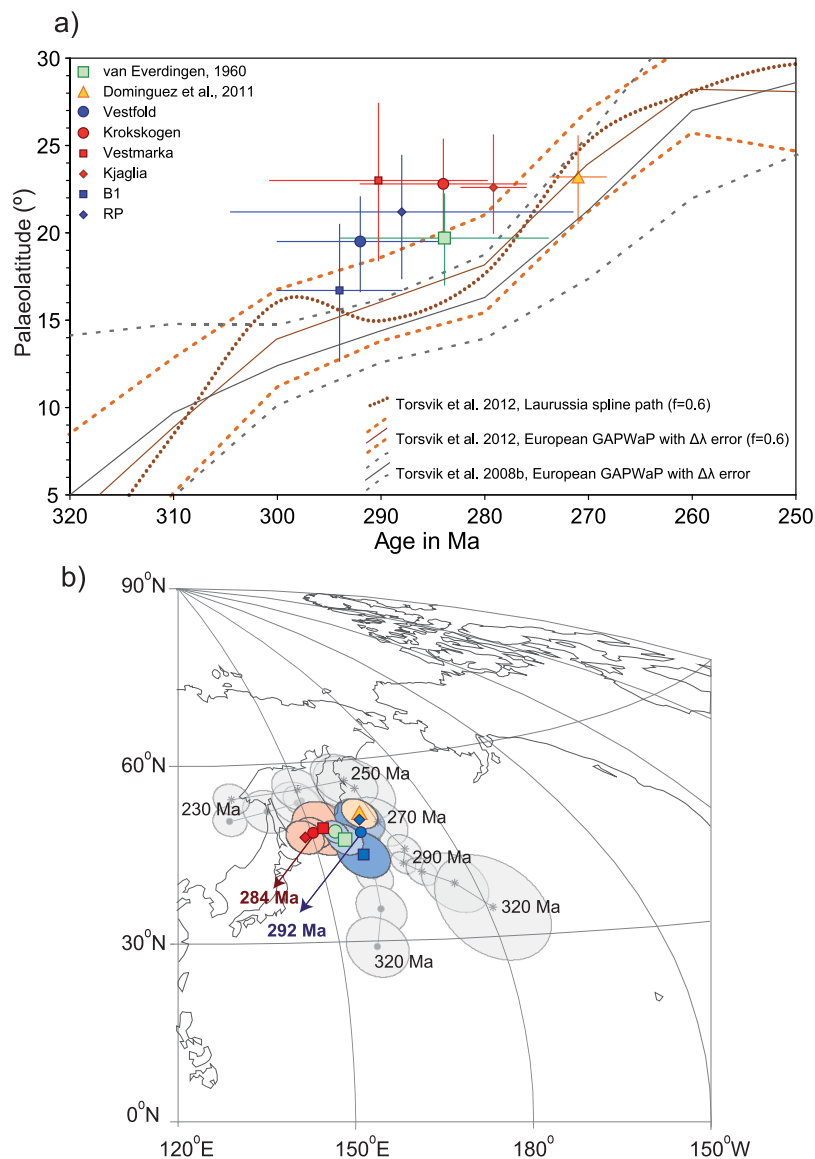


Figure 9. (a) Plot of palaeolatitude versus age showing the predicted palaeolatitude (dark grey line) according to Torsvik *et al.* (2008b) and in dark brown according to Torsvik *et al.* (2012) for the Oslo Graben (60°N, 10°E) and the error bounds (dashed grey/brown lines) based on the error in inclination (ΔI_x) derived from A_{95} . Dotted brown curve represents the recommended Laurussian spline path from Torsvik *et al.* (2012). (b) Aitoff projection of the apparent polar wander path (APWP) in grey with corresponding A_{95} circles for the age interval 320–230 Ma (in 10 Ma increments) according to Torsvik *et al.* (2008b; asterisks) and Torsvik *et al.* (2012; closed circles). Remaining symbols are the same as in (a).

(e.g. Torsvik *et al.* 2006; Alvey 2009; Labails *et al.* 2010) show that Pangaea A reconstructions are possible without the necessity of introducing non-dipolar fields. The question remains however, if it is valid to introduce a uniform flattening factor for all sediments, as flattening factors have been shown to vary widely in both magnetite and hematite bearing rocks (Bilardello & Kodama 2010). Applying a blanket flattening factor is however possibly the best approach currently at hand.

Very recently, new studies have become available that present large high-quality data sets, often corrected for inclination shallowing whenever sediments were the subject of research. Studies on both the Laurussian (Iosifidi *et al.* 2010; Meijers *et al.* 2010; Dominguez *et al.* 2011; Yuan *et al.* 2011) and Gondwana part of Pangaea (Domeier *et al.* 2011) conclude in favour of Pangaea A-type reconstructions. The higher palaeolatitudes from our study

and the study by Dominguez *et al.* (2011) from the Oslo Graben would not necessitate a Pangaea B type reconstruction in the early Permian, when comparing the poles to the latest APWPs (Torsvik *et al.* 2008b, 2012; Figs 10a and b). This is in line with recent studies carried out on volcanics and sediments (corrected for inclination shallowing) from other parts of Europe. Yuan *et al.* (2011) present data from lower Permian trachytes from the Ukrainian shield, which is part of the East European Craton. On the basis of their data a Pangaea A-type reconstruction is favoured. Meijers *et al.* (2010) present a large data set of Carboniferous and lowermost Permian sediments from the Donbas Foldbelt; an inverted rift basin that is part of the East European Craton. All sites, except for the earliest Permian site were corrected for inclination shallowing with the TK03.GAD model (Tauxe & Kent 2004), and also conclude that there is no necessity for Pangaea B. In all these cases however, using the mean

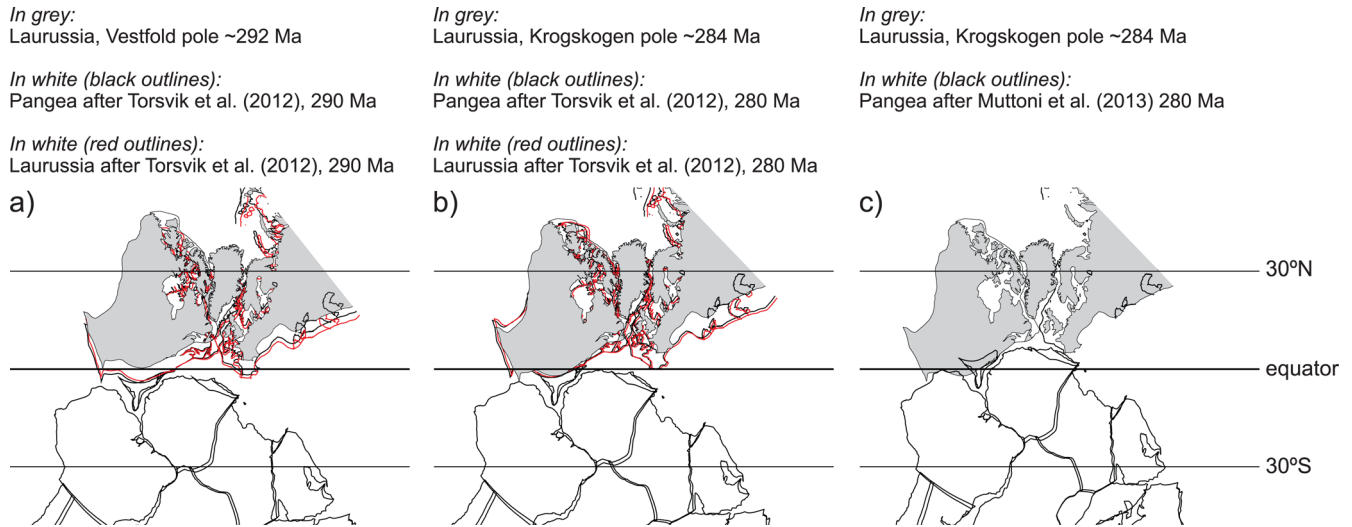


Figure 10. Palaeogeographic reconstructions of Laurussia based on our data (in grey). Pangaea reconstructions in (a) (~292 Ma) and (b) (~284 Ma) are constructed according to the recommended GAPWaP path (black outlines) as presented in tables 10 and 11 of Torsvik *et al.* (2012) that assumes a uniform flattening factor of 0.6 for all included sedimentary data sets that were not corrected for inclination shallowing in the original publications. Additional Laurussia reconstructions (red outlines) are shown based on the recommended spherical spline APWP for Laurussia as presented in table 5 of Torsvik *et al.* (2012). (c) Gondwana reconstruction based on Muttoni *et al.* (2013). The combination of our Laurussia reconstruction and the Muttoni *et al.* (2013) Gondwana reconstruction leads to a small overlap of the major continents (present-day North America and South America) and a more problematic fit of present-day Florida. The position of Laurentia was reconstructed using an Euler pole at 78.6°N, 161.9°E (angle = 31.0°) following Torsvik *et al.* (2006) and Domeier *et al.* (2012).

pole for Gondwana as presented by Muttoni *et al.* (2013) would lead to an overlap between the northern and southern continents, leading to a Pangaea B type reconstruction. Yuan *et al.* (2011) therefore correctly conclude that one will have to omit the data from Adria in order to allow a Pangaea A reconstruction unless the position of Adria with respect to Africa is not rigid (*cf.* Van Hinsbergen *et al.* 2014).

Pangaea B reconstructions are supported by two studies carried out in the Laurasian part of Pangaea (present-day eastern Canada; Bilardello & Kodama 2009, 2010; Kodama 2009). Sediments from those two studies corrected for inclination shallowing using the method of Tan & Kodama (2003) result in higher southerly latitudes for the portion of Laurussia located on the southern hemisphere in the Carboniferous, therefore increasing the overlap between Laurussia and Gondwana. Interestingly, the vast majority of Laurussia was located on the southern hemisphere in the early Carboniferous. Its northward drift led to the position of most of the continental Laurussian landmass on the northern hemisphere by the late Carboniferous. Overall, correcting poles derived from sediments from both sides of the equator for inclination shallowing therefore inevitably leads to symmetric stretching of Laurussia around the equator, which poses an interesting issue.

In concurrence with Yuan *et al.* (2011) we conclude that the crux in the current Pangaea A versus B debate lies in data selection and reliability criteria. The solution to the ongoing controversy is likely hidden in geological records from the southern continents that were assembled in Gondwana. Increasing the limited number of high-quality data sets from Gondwana is however a challenging task since the records have often been affected by remagnetization (e.g. Font *et al.* 2012). A start could be made by correcting individual sedimentary data sets for inclination shallowing rather than applying blanket flattening factors for many of the studies included in Torsvik *et al.* (2012) and by increasing the sampling size and establishing

new ages for the individual poles that were combined to a mean pole for Gondwana by Muttoni *et al.* (2013).

5 GEOMAGNETIC FIELD BEHAVIOUR OF THE OSLO GRABEN VOLCANICS DURING THE PCRS

Superchrons as long, stable intervals of the same polarity are intriguing features of the Earth's magnetic field, with durations of tens of millions of years and thus comparable to timescales of mantle processes and plate tectonics. These long periods that the geodynamo is in a non-reversing state are particularly interesting because they may imply distinctly different and very long-term physical processes that influence the geodynamo. Biggin *et al.* (2008b) analysed geomagnetic palaeosecular variation (PSV) in the period 2.45–2.82 Gyr and concluded that PSV was fundamentally different from that observed for the last 5 Myr (McElhinny & McFadden 1997) and the last 200 Myr (McFadden *et al.* 1991). Their conclusion suggested that geomagnetic reversals were likely much less common in the late Archaean than over the past 5 Myr (Johnson *et al.* 2008). The results of geodynamo simulations seem to indicate that this enhanced stability could be a consequence of a smaller (or absent) inner core at this time (Roberts & Glatzmaier 2001; Coe & Glatzmaier 2006). A more recent modelling study (Aubert *et al.* 2009) has largely corroborated this while indicating that the inner core may influence the geodynamo more through its effect on the available convective power than through its effect on outer core geometry. Significantly lower VGP scatter at low latitudes during superchrons was observed both in the CNS from a compilation of volcanic data (Biggin *et al.* 2008a) and in the PCRS from a compilation of data from red beds in two basins in southern France (Haldan *et al.* 2009). In Fig. 11(a), we compare the VGP scatter (S) from the Oslo Graben

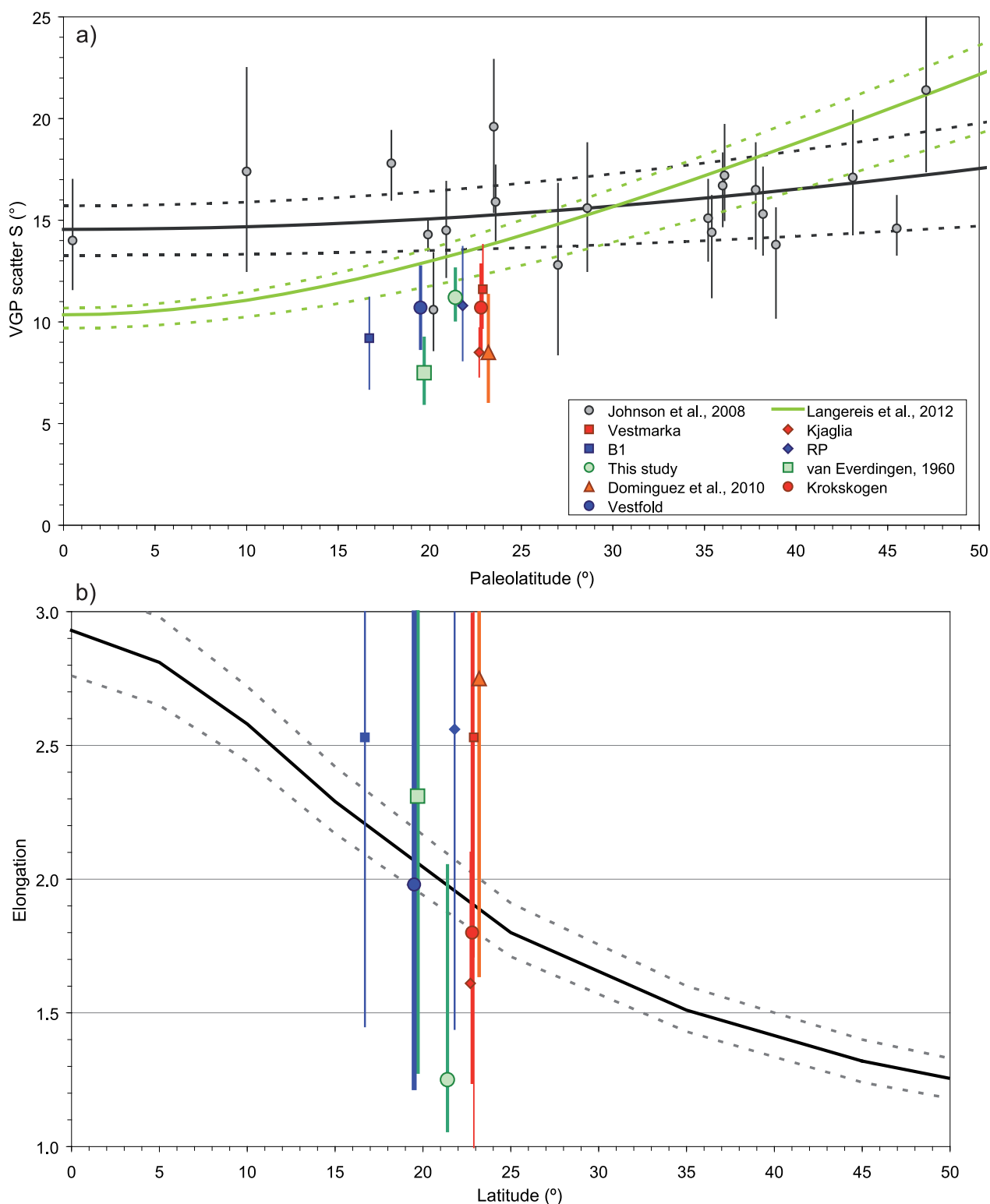


Figure 11. (a) VGP scatter versus palaeolatitude of the data sets. The black line shows the Model G (McFadden *et al.* 1988) approach through the data (light grey circles) of Johnson *et al.* (2008) for the last 5 Myr. Model G is a phenomenological model of PSV, which uses two ‘shape parameters’ to define a quadratic curve, which is then fit (by the least-squares technique) to a set of VGP scatter data plotted against (palaeo)latitude. We used a bootstrap method where each of the 1000 bootstraps takes a random sample within the published error limits of each individual data point (Haldan *et al.* 2009). The green line represents a best-fitting Model G of the sedimentary data compilation from the PCRS of Langereis *et al.* (2012). (b) Elongation versus latitude (black line) plus 95 per cent bootstrap error bounds (dashed lines), predicted according to the TKO3.GAD field model (Tauxe & Kent 2004). Symbols are explained in the legend of Fig. 11(a).

with the VGP scatter of the last 5 Myr of Johnson *et al.* (2008) and with the PCRS (Langereis *et al.* 2012). The VGP scatter from the Oslo Graben is shown without any cut-off, since both a 45° and variable cut-off (Vandamme 1994) did not exclude any data points. The VGP scatter of the Oslo Graben volcanics is lower than that of the last 5 Myr, but indistinguishable if compared to the sedimentary PCRS compilation (Langereis *et al.* 2012). More in particular, the VGP scatter from the distributions of the Krokstogen and Vestfold areas are near-identical. Likely, this is caused by the large data set ($N = 104$) which sample secular variation over a sufficiently long time, whereas the scatter of the individual formations may each represent a too small distribution, and therefore underestimate S . We also note that if we average the two areas into a single Oslo Graben distribution, the VGP scatter compares well with the PCRS compilation (Langereis *et al.* 2012), while the scatter from the data of van Everdingen (1960) is statistically significantly lower. Again, this is likely caused by a too small data set ($N = 27$). In any case, the data from the Oslo Graben seem to confirm that during a superchron PSV is significantly lower at low latitudes than found during times of frequent reversals (Biggin *et al.* 2008a; Haldan *et al.* 2009).

We also compared the elongation (E) of the distributions from the Oslo Graben with the expected values from the TK03.GAD statistical field model (Tauxe & Kent 2004). Observations from five Large Igneous Provinces (LIPs) of the early Cretaceous age and younger (Yemen, Kerguelen, Faroe Islands, Deccan and Paraná basalts; Tauxe *et al.* 2008) and from ancient (1.1 Ga) Keweenaw lava flows Tauxe & Kodama 2009) showed that the distributions—in terms of E/I trends—are consistent at the 95 per cent level with the predictions from the model. A requirement for a reliable comparison with the model is a sufficiently large sample set: for a distribution smaller than 100 samples, the results are less reliable. If we compare the elongation of the Oslo Graben data (Fig. 11b) with the predicted trend in elongation, we find that the elongation of both the Krokstogen and Vestfold area agree very well. The elongation of the four formations show widely varying values of E , but are mostly too high, probably because they do not meet the minimum required number of samples. Combining the two areas into a single Oslo Graben value causes a much lower E value than predicted by TK03.GAD, due to the declination difference between the two areas: this will cause the distribution to become more elongated in the E–W direction, thereby reducing the expected (N–S) elongation at this latitude. However, every distribution fits the predicted elongation within their 95 per cent bootstrap errors which are very large. Although determining elongation of a particular distribution and comparing it to a field model like TK03.GAD is a useful extra test, it seems that VGP scatter is a more sensitive and discriminating parameter to test a distribution.

6 CONCLUSIONS

We have performed an extended palaeomagnetic study of the Oslo Graben volcanics, compared to the study of more than half a century ago by van Everdingen (1960), using modern techniques and a four times larger amount of sites (104 versus 27). We must conclude that the average direction (and palaeomagnetic pole) of the Krokstogen and Vestfold volcanics together are statistically identical to those of the earlier study. This gives confidence in the fact that older palaeomagnetic studies can be reliable and robust, even though methods have improved. Our larger number of sites, and better available age constraints, however, allow us to separate the data into two major intervals, of the on average younger Krokstogen area and

the older Vestfold area. The results are a valuable addition to the Permian database of Laurussia and show firstly that palaeolatitudes are slightly higher—though within error—compared to most recent APWP of Torsvik *et al.* (2012). This implies that for both the early Permian and the late Permian (Dominguez *et al.* 2011) a Pangaea B configuration is not required, based on data from the Oslo Graben. The mean 280 Ma pole for Gondwana presented by Muttoni *et al.* (2003, 2009, 2013) would lead to a slight overlap between Laurentia and South America, but is mostly problematic for Florida, therefore necessitating Pangaea B.

The larger sample size also allows assessing the distributions of directions of the Oslo Graben—acquired during a superchron, the PCRS—in terms of geomagnetic field behaviour. In particular, the distributions show a significantly lower VGP scatter at the observed (low) latitudes than expected from a compilation of the last 5 Myr (Johnson *et al.* 2008) but show excellent agreement with the scatter observed both during the CNS (Biggin *et al.* 2008a) and during the PCRS (Langereis *et al.* 2012). A comparison of the distributions in terms of elongation is less discriminating, since the large errors in all cases allow a fit to the predicted elongation/inclination behaviour of the TK03.GAD model. Nevertheless, the elongation of the two areas, Krokstogen and Vestfold, fit the predicted values remarkably well, although the entire Oslo Graben distribution does not.

ACKNOWLEDGEMENTS

We thank Martijn Deenen and Mark Dekkers for their help in the field and for constructive discussions and the late Tom Mullender for technical support. This work was funded by the Netherlands Organization for Scientific Research (NWO). MJMM acknowledges funding and support from the Henri Poincaré Fellowship (Observatoire de la Côte d'Azur, Nice) and the College of Science and Engineering and the Department of Earth Sciences at the University of Minnesota. The manuscript benefited from the reviews of Conall Mac Niocaill and an anonymous reviewer.

REFERENCES

- Alvey, A., 2009. Using crustal thickness and continental lithosphere thinning factors from gravity inversion to refine plate reconstruction models for the Arctic & North Atlantic, *PhD thesis*, University of Liverpool, 189 pp.
- Angiolini, L., Gaetani, M., Muttoni, G., Stephenson, M.H. & Zanchi, A., 2007. Tethyan oceanic currents and climate gradients 300 m.y. ago, *Geology*, **35**(12), 1071–1074.
- Arthaud, F. & Matte, P., 1977. Late Paleozoic strike-slip faulting in southern Europe and northern Africa: result of a right-lateral shear zone between the Appalachians and the Urals, *Bull. geol. Soc. Am.*, **88**, 1305–1320.
- Aubert, J., Labrosse, S. & Poitou, C., 2009. Modeling the palaeo-evolution of the geodynamo, *Geophys. J. Int.*, **179**, 1414–1428.
- Besse, J. & Courtillot, V., 2002. Apparent and true polar wander and the geometry of the geomagnetic field in the last 200 million years, *J. geophys. Res.*, **107**(B11), doi:10.1029/2000JB000050.
- Biggin, A.J., Van Hinsbergen, D.J.J., Langereis, C.G., Straathof, G.B. & Deenen, M.H.L., 2008a. Geomagnetic secular variation in the Cretaceous Normal Superchron and in the Jurassic, *Phys. Earth planet. Inter.*, **169**, 3–19.
- Biggin, A.J., Strik, G.H.M.A. & Langereis, C.G., 2008b. Evidence for a very-long-term trend in geomagnetic secular variation, *Nat. Geosci.*, **1**(6), 395–398.
- Bilardello, D. & Kodama, K.P., 2009. Palaeomagnetism and magnetic anisotropy of Carboniferous red beds from the Maritime Provinces of

- Canada: evidence for shallow palaeomagnetic inclinations and implications for North American apparent polar wander, *Geophys. J. Int.*, **180**, 1013–1029.
- Bilardello, D. & Kodama, K.P., 2010. Rock magnetic evidence for inclination shallowing in the early Carboniferous Deer Lake Group red beds of western Newfoundland, *Geophys. J. Int.*, **181**, 275–289.
- Butler, R.F., 1992. *Paleomagnetism: Magnetic Domains to Geologic Terranes*, Blackwell Scientific Publications, 319 pp.
- Coe, R.S. & Glatzmaier, G.A., 2006. Symmetry and stability of the geomagnetic field, *Geophys. Res. Lett.*, **33**(21), doi:10.1029/2006GL027903.
- Constable, C.G. & Parker, R.L., 1988. Statistics of the geomagnetic secular variation for the past 5 m.y., *J. geophys. Res.*, **93**, 11 569–11 581.
- Corfu, F. & Dahlgren, S., 2008. Perovskite U–Pb ages and the Pb isotopic composition of alkaline volcanism initiating the Permo-Carboniferous Oslo Rift, *EPSL*, **265**, 256–269.
- Creer, K.M., Irving, E. & Runcorn, S.K., 1954. The direction of the geomagnetic field in remote epochs in Great Britain, *J. Geomag. Geoelectr.*, **6**, 163–168.
- Creer, K.M., Irving, E. & Nairn, A.E.M., 1959. Paleomagnetism of the Great Whin Sill, *Geophys. J. R. astr. Soc.*, **2**, 306–323.
- Dankers, P.H.M., 1978. Magnetic properties of dispersed natural iron-oxides of known grain size, *PhD thesis*, Utrecht University.
- De Boer, C.B. & Dekkers, M.J., 2001. Unusual thermomagnetic behaviour of haematites: neof ormation of a highly magnetic spinel phase on heating in air, *Geophys. J. Int.*, **144**, 481–494.
- Deenen, M.H.L., Langereis, C.G., Van Hinsbergen, D.J.J. & Biggin, A.J., 2011. Geomagnetic secular variation and the statistics of palaeomagnetic directions, *Geophys. J. Int.*, **186**, 509–520.
- Dietz, R.S., 1961. Continent and ocean basin evolution by spreading of the sea floor, *Nature*, **190**, 854–857.
- Domeier, M., Van der Voo, R., Tomezzoli, R.N., Tohver, E., Hendriks, B.W.H., Torsvik, T.H., Vizan, H. & Dominguez, A., 2011. Support for an “A-type” Pangea reconstruction from high-fidelity Late Permian and Early to Middle Triassic palaeomagnetic data from Argentina, *J. geophys. Res.*, **116**, B12114, doi:10.1029/2011JB008495.
- Domeier, M., Van der Voo, R. & Torsvik, T.H., 2012. Paleomagnetism and Pangea: the road to reconciliation, *Tectonophysics*, **514–517**, 14–43.
- Dominguez, A.R., Van der Voo, R., Torsvik, T.H., Hendriks, B.W.H., Abrajevitch, A., Domeier, M., Larsen, B.T. & Rousse, S., 2011. The 270 Ma paleolatitude of Baltica and its significance for Pangea models, *Geophys. J. Int.*, **186**, 529–550.
- Du Toit, A.L., 1937. *Our Wandering Continents*, Oliver and Boyd.
- Fisher, D.A., 1953. Dispersion on a sphere, *Proc. R. Soc. Lond., A*, **217**, 295–305.
- Font, E., Rapalini, A.E., Tomezzoli, R.N., Trindade, R.I.F. & Tohver, E., 2012. Episodic remagnetizations related to tectonic events and their consequences for the South America Polar Wander Path, in *Remagnetization and Chemical Alteration of Sedimentary Rocks*, pp. 55–87, eds Elmore, R.D., Muxworthy, A.R., Aldana, M.M. & Mena, M., The Geological Society of London, Special Publications 371.
- Grommé, S., Wright, T.L. & Peck, D.L., 1969. Magnetic properties and oxidation of iron-titanium oxide minerals in Alae and Makaopuhi lava lakes, Hawaii, *J. geophys. Res.*, **74**, 5277–5294.
- Gutierrez-Alonso, G., Fernandez-Suarez, J., Weil, A.B., Murphy, J.B., Nance, R.D., Corfu, F. & Johnston, S.T., 2008. Self-subduction of the Pangaean global plate, *Nat. Geosci.*, **1**, 549–553.
- Haldan, M.M., Langereis, C.G., Biggin, A.J., Dekkers, M.J. & Evans, M.E., 2009. A comparison of detailed equatorial red bed records of secular variation during the Permo-Carboniferous Reversed Superchron, *Geophys. J. Int.*, **177**(3), 834–848.
- Heeremans, M., Larsen, B.T. & Stel, H., 1997. Paleostress reconstruction from kinematic indicators in the Oslo Graben, southern Norway: new constraints on the model of rifting, *Tectonophysics*, **266**, 55–79.
- Heezen, B.C., 1960. The rift in the ocean floor, *Scient. Am.*, **203**, 98–110.
- Heslop, D., McIntosh, G. & Dekkers, M.J., 2004. Using time- and temperature-dependent Preisach models to investigate the limitations of modeling isothermal remanent magnetisation acquisition curves with cumulative log Gaussian functions, *Geophys. J. Int.*, **157**, 55–63.
- Iosifidi, A.G., Mac Niocail, C., Khramov, A.N., Dekkers, M.J. & Popov, V.V., 2010. Palaeogeographic implications of differential inclination shallowing in permo-carboniferous sediments from the Donets basin, Ukraine, *Tectonophysics*, **490**, 229–240.
- Irving, E., 1977. Drift of the major continental blocks since the Devonian, *Nature*, **270**, 304–309.
- Johnson, C.L. et al., 2008. Recent investigations of the 0–5 Ma geomagnetic field recorded by lava flows, *Geochem. Geophys. Geosyst.*, **9**, Q04032, doi:10.1029/2007GC001696.
- Kent, D.V. & Smethurst, M.A., 1998. Shallow bias of paleomagnetic inclinations in the Paleozoic and Precambrian, *Earth planet. Sci. Lett.*, **160**, 391–402.
- Kirschvink, J.L., 1980. The least-square line and plane and the analysis of paleomagnetic data, *Geophys. J. R. astr. Soc.*, **62**, 699–718.
- Kodama, K.P., 2009. Simplification of the anisotropy-based inclination correction technique for magnetite- and haematite-bearing rocks: a case study for the Carboniferous Glenshaw and Mauch Chunk Formations, North America, *Geophys. J. Int.*, **176**(2), 467–477.
- Köppen, W. & Wegener, A., 1924. *Die Klimate der geologischen Vorzeit*, Berlin.
- Kruiver, P.P., Dekkers, M.J. & Heslop, D., 2001. Quantification of magnetic coercivity components by the analysis of acquisition curves of isothermal remanent magnetisation, *Earth planet. Sci. Lett.*, **189**, 269–276.
- Labails, C., Olivet, J.L., Aslanian, D. & Roest, W.R., 2010. An alternative early opening scenario for the Central Atlantic Ocean, *Earth planet. Sci. Lett.*, **297**(3–4), 355–368.
- Langereis, C.G., Haldan, M. & Biggin, A.J., 2012. Paleosecular variation during the Permo-Carboniferous Reversed Superchron: a comparison between the sedimentary and volcanic record (abstract), in *Proceedings of the GP11A-04, 2012 Fall Meeting*, AGU, San Francisco, CA, 3–7 Dec.
- Larsen, B.T., 1978. Krokstogen Lava area. The Oslo Paleorift. A review guide to excursions, *Norsk Geol. Unders.*, **337**, 143–162.
- Larsen, B.T. & Olausson, S., 2005. The Oslo Region. A study in classical Paleozoic Geology, *Norsk Geologisk Forening*, 1–88.
- Larsen, B.T. & Sundvoll, B.A., 1984. The Oslo Graben: a high-volcanicity continental rift (abstract), *EOS, Trans. geophys. Am. Un.*, **65**, 1084.
- McElhinny, M.W. & McFadden, P.L., 1997. Palaeosecular variation over the past 5 Myr based on a new generalized database, *Geophys. J. Int.*, **131**(2), 240–252.
- McFadden, P.L. & McElhinny, M.W., 1990. Classification of the reversal test in palaeomagnetism, *Geophys. J. Int.*, **103**, 725–729.
- McFadden, P.L., Merrill, R.T. & McElhinny, M.W., 1988. Dipolequadrupole family modeling of paleosecular variation, *J. geophys. Res.*, **93**(B10), 11 583–11 588.
- McFadden, P.L., Merrill, R.T., McElhinny, M.W. & Lee, S., 1991. Reversals of the Earth’s magnetic field and temporal variations of the dynamo families, *J. geophys. Res. B: Solid Earth*, **96**, 3923–3933.
- Meijers, M.J.M., Hamers, M.F., van Hinsbergen, D.J.J., van der Meer, D.G., Kitchka, A., Langereis, C.G. & Stephenson, R.A., 2010. New late Paleozoic paleopoles from the Donbas Foldbelt (Ukraine): implications for the Pangea A vs. B controversy, *Earth planet. Sci. Lett.*, **297**(18–33), doi:10.1016/j.epsl.2010.05.028.
- Morel, P. & Irving, E., 1981. Paleomagnetism and the Evolution of Pangea, *J. geophys. Res.*, **86**(B3), 1858–1872.
- Mullender, T.A.T., van Velzen, A.J. & Dekkers, M.J., 1993. Continuous drift correction and separate identification of ferromagnetic and paramagnetic contributions in thermomagnetic runs, *Geophys. J. Int.*, **114**, 663–672.
- Müller, R.D., Royer, J.-Y. & Lawver, L.A., 1993. Revised plate motions relative to the hotspots from combined Atlantic and Indian Ocean hotspot tracks, *Geology*, **21**(3), 275–278.
- Muttoni, G., Kent, D.V., Garzanti, E., Brack, P., Abrahamsen, N. & Gaetani, M., 2003. Early Permian Pangea ‘B’ to Late Permian Pangea ‘A’, *Earth planet. Sci. Lett.*, **215**, 379–394.

- Muttoni, G. *et al.*, 2009. Opening of the Neo-Tethys Ocean and the Pangea B to Pangea A transformation during the Permian, *GeoArabia*, **14**(4), 17–48.
- Muttoni, G., Dallanave, E. & Channell, J.E.T., 2013. The drift history of Adria and Africa from 280 Ma to Present, Jurassic true polar wander, and zonal climate control on Tethyan sedimentary facies, *Palaeogeogr., Palaeoclimatol., Palaeoecol.*, **386**, 415–435.
- Neumann, E.R., Dunworth, E.A., Sundvoll, B.A. & Tollefsrud, J.I., 2002. B-1 basaltic lavas in Vestfold-Jeloya area, central Oslo rift: derivation from initial melts formed by progressive partial melting of an enriched mantle source, *Lithos*, **61**(1–2), 21–53.
- Norton, I.O., 2000. Global hotspot reference frames in plate motion, in *The History and Dynamics of Global Plate Motion*, pp. 339–357, eds Richards, M.A., Gordon, R.G. & van der Hilst, R.D., AGU.
- Olaussen, S., Larsen, B.T. & Steel, R., 1994. The Upper Carboniferous-Permian Oslo Rift: basin fill in relation to tectonic development, *Can. Soc. Petr. Geol., Memoir*, **17**, 175–197.
- Richards, M.A., Duncan, R.A. & Courtillot, V.E., 1989. Flood basalts and hotspot tracks: plume heads and tails, *Science*, **246**, 103–107.
- Roberts, P.H. & Glatzmaier, G.A., 2001. The geodynamo, past, present and future, *Geophys. Astrophys. Fluid Dyn.*, **94**, 47–84.
- Rochette, P. & Vandamme, D., 2001. Pangea B: an artifact of incorrect paleomagnetic assumptions?, *Ann. Geof.*, **44**(3), 649–658.
- Schaltegger, U. & Brack, P., 2007. Crustal-scale magmatic systems during intracontinental strike-slip tectonics: U, Pb and Hf isotopic constraints from Permian magmatic rocks of the Southern Alps, *Int. J. Earth Sci.*, **96**, 1131–1151.
- Storetvedt, K.M., Pedersen, S., Lovlie, R. & Halvorsen, E., 1978. Paleomagnetism in the Oslo Rift zone, in *Tectonics and Geophysics of Continental Rifts*, pp. 289–296, eds Ramberg, J.B. & Neumann, E.R., D. Reidel Publ. Co.
- Sundvoll, B. & Larsen, B.T., 1990. Rb-Sr isotope systematics in the magmatic rocks of the Oslo Rift, *Nor. Geol. Unders. Bull.*, **418**, 25–41.
- Sundvoll, B., Larsen, B.T. & Wandaas, B., 1992. Early Magmatic Phase in the Oslo Rift and Its Related Stress Regime, *Tectonophysics*, **208**(1–3), 37–54.
- Tan, X. & Kodama, K.P., 2003. An analytical solution for correcting paleomagnetic inclination error, *Geophys. J. Int.*, **152**, 228–236.
- Tauxe, L. & Kent, D.V., 2004. A simplified statistical model for the geomagnetic field and the detection of shallow bias in paleomagnetic inclinations: was the ancient magnetic field dipolar?, *Geophys. Monogr.*, **145**, 101–116.
- Tauxe, L. & Kodama, K.P., 2009. Paleosecular variation models for ancient times: clues from Keweenaw lava flows, *Phys. Earth planet. Inter.*, **177**, 31–45.
- Tauxe, L. & Watson, G.S., 1994. The foldtest: an eigen analysis approach, *Earth planet. Sci. Lett.*, **122**, 331–341.
- Tauxe, L., Kodama, K.P. & Kent, D.V., 2008. Testing corrections for paleomagnetic inclination error in sedimentary rocks: a comparative approach, *Phys. Earth planet. Inter.*, **169**, 152–165.
- Torqu, F., Besse, J., Vaslet, D., Marcoux, J., Ricou, E., Halawani, M. & Basahel, M., 1997. Paleomagnetic results from Saudi Arabia and the Permo-Triassic Pangea configuration, *Earth planet. Sci. Lett.*, **148**, 553–567.
- Torsvik, T.H., Gaina, C., Steinberg, M. & Van der Voo, R., 2006. North Atlantic fits with implications for the Barents Sea, Norwegian Geol. Survey Industry Report (confidential).
- Torsvik, T.H., Steinberger, B., Cocks, L.R.M. & Burke, K., 2008a. Longitude: Linking Earth's ancient surface to its deep interior, *Earth planet. Sci. Lett.*, **276**, 273–282.
- Torsvik, T.H., Muller, R.D., Van Der Voo, R., Steinberger, B. & Gaina, C., 2008b. Global plate motion frames: toward a unified model, *Rev. Geophys.*, **46**, RG3004, doi:10.1029/2007RG000227.
- Torsvik, T.H. *et al.*, 2012. Phanerozoic polar wander, palaeogeography and dynamics, *Earth-Sci. Rev.*, **114**(3–4), 325–368.
- Van der Voo, R. & Torsvik, T.H., 2001. Evidence for late Paleozoic and Mesozoic nondipole fields provides an explanation for the Pangea reconstruction problems, *Earth planet. Sci. Lett.*, **187**, 71–81.
- Van der Voo, R. & Torsvik, T.H., 2004. The quality of the European Permo-Triassic paleopoles and its impact on Pangea reconstructions, in *Timescales of the Internal Geomagnetic Field*, pp. 29–42, eds Channell, J.E.T., Kent, D.V., Lowrie, W. & Meert, J.G., AGU Geophysical Monograph 145.
- Van Everdingen, R.O., 1960. Paleomagnetic analysis of Permian extrusives in the Oslo region, Norway. Studies on the Igneous Rock Complex of the Oslo Region, *PhD thesis*, Skr. Nor. Vidensk. - Akad. Oslo, XVII(1), 1–80.
- Van Hinsbergen, D.J.J., Mensink, M., Langereis, C.G., Maffione, M., Spalluto, L., Tropeano, M. & Sabato, L., 2014. Did Adria rotate relative to Africa? *Solid Earth*, **5**, 611–629.
- Vandamme, D., 1994. A new method to determine paleosecular variation, *Phys. Earth planet. Int.*, **85**, 131–142.
- Watson, G., 1983. Large sample theory of the Langevin distributions, *J. Stat. Plann. Infer.*, **8**, 245–256.
- Wegener, A.L., 1915. *Die Entstehung der Kontinente und Ozeane*, Braunschweig Vieweg, 94 pp.
- Yuan, K., Van der Voo, R., Bazhenov, M.L., Bakhmutov, V., Alekhin, V. & Hendriks, B.W.H., 2011. Permian and Triassic palaeolatitudes of the Ukrainian shield with implications for Pangea reconstructions, *Geophys. J. Int.*, **184**, 595–610.
- Zijderveld, J.D.A., 1967. A. C. demagnetisation of rocks: analysis of results, in *Methods in Palaeomagnetism*, pp. 254–286, eds Collinson, D.W., Creer, K.M. & Runcorn, S.K., Elsevier.

SUPPORTING INFORMATION

Additional Supporting Information may be found in the online version of this article:

Table S1. Palaeomagnetic data per site. Formation (Fm, Vm = Vestmarka, Kj = Kjaglia, VF = Vestfold), group (1–6 in Kroksko-gen, B1, RP series in Vestfold), N_c = number of cores taken, site name, longitude and latitude (long, lat), N = number of cores successfully demagnetized, mean declination, inclination (dec, inc) and Fisher parameters (k , α_{95}), bedding and strike plus tilt corrected directions (dece_tc, inc_tc). Double asterisk (**) means that the site gave no results or was rejected. (<http://gji.oxfordjournals.org/lookup/suppl/doi:10.1093/gji/ggu351/-/DC1>)

Please note: Oxford University Press is not responsible for the content or functionality of any supporting materials supplied by the authors. Any queries (other than missing material) should be directed to the corresponding author for the article.